UNIVERSITA' DEGLI STUDI DI VERONA

DIPARTIMENTO DI

PATOLOGIA e DIAGNOSTICA

SCUOLA DI DOTTORATO DI

SCIENZE BIOMEDICHE TRASLAZIONALI

DOTTORATO DI RICERCA IN

PATOLOGIA ONCOLOGICA E CELLULE STAMINALI

CICLO XXVI

CLEAR CELL-PAPILLARY RENAL CELL CARCINOMA

S.S.D. MED/08

Coordinatore: Prof. Aldo SCARPA

Tutor: Prof. Marco CHILOSI

Dottorando: Dott. Stefano GOBBO

INTRODUCTION

The classification of renal cell neoplasms includes numerous entities characterized by different prognosis and the correct subtyping is one of the most important procedures to predict the behavior of these tumors.[1-5] Clear cell renal cell carcinoma (RCC) that in 20% of cases shows metastases at the time of the diagnosis and in 30-40% develops metastases during the follow up period, represents the majority of renal cell tumors. However, other renal cell carcinomas with lower malignancy or benign renal cell neoplasms can occur. Due to overlapping morphological features and the increasing recognition of novel entities[6], the histologic distinction of renal cell neoplasms is becoming challenging or sometime insufficient. That is why traditional histology needs today the support of more specific tools making the correct classification more and more feasible and reproducible. Different subtypes of renal cell tumors are identified by specific molecular markers that often represent the most reliable aspect of them and sometime the unique specific feature[7]. Several markers have been proposed as distinctive features suggesting a role of the protein expression profile and cytogenetic pattern in the recognition and classification of renal cell tumors.[7-10] Since paraffin embedded tissue is the most diffuse available material in pathology laboratories, the immunohistochemistry and fluorescence in situ hybridization analyses have become the most powerful tools able to obtain the protein and cytogenetic expression profiling of these neoplasms.

Moreover, targeted therapies, such as the novel tyrosine kinase inhibitors Sunitinib and Sorafenib have been approved by the Food and Drug Administration as having significant clinical activity in metastatic clear cell renal cell carcinoma.[11]

Different types of renal epithelial neoplasms have been described in association with end-stage renal disease, with a high prevalence of papillary renal cell

carcinomas and clear cell renal cell carcinomas.[12-20] However, tumors arising in kidneys involved by end-stage renal diseases may also show distinctive histologic features not easily classified according to the current WHO classification system.[21-23] In 2006 two distinctive renal carcinomas have been described in the spectrum of epithelial neoplasms in end-stage renal disease. The most common was designated as "acquired cystic disease associated renal carcinoma" and the second as "clear-cell papillary renal cell carcinoma of the end-stage kidneys". The latter is a tumor composed mainly of cells with clear cytoplasm arranged in cystic and papillary patterns.[23]

Acquired cystic disease-associated renal cell carcinoma is generally positive for vinculin and parvalbumin and showed a strong and diffuse immunoexpression for AMACR, whereas CK7 was negative.[23] Cossu-Rocca et al. found that eosinophilic renal cell tumors associated with acquired cystic disease have genetic profiles distinct from the renal cell neoplasms recognized in the current classification. They showed no losses or gains of chromosomes 1, 2, 6, 10, or 17 in one tumor and gains of chromosomes 1, 2, and 6 in other two tumors.[24] Recently, O'Reilly et al described in abstract form FISH analyses with centromeric probes for chromosomes 1, 3, 7 and 17 on 10 tumors arising in end-stage renal disease, among which two acquired cystic kidney disease-associated tumors were included. They found that both tumors were disomic for chromosomes 1 and 3, whereas one had loss of chromosome 7 and the other showed loss of chromosome 17.[25]

Clear-cell papillary renal cell carcinoma of the end-stage kidney described by Tickoo et al., unlike papillary RCC, were constantly negative for AMACR, but unlike clear-cell RCC all tumors tested showed strong immunoexpression for CK7.[23]

In 2008 we found similar results studying clear-cell papillary renal cell carcinomas arising in normal kidneys. We observed also the positive immunoreaction for CA9 and the lack of immunoexpression of CD10 and TFE3. Cytogenetically, clear-cell papillary renal cell carcinomas were characterized by the absence of the typical chromosomal aberrations found in papillary RCC (trisomy of chromosome 7 and 17 and loss of chromosome Y) or in clear cell RCC (deletion of chromosome 3p).[26]

These findings let us to identify clear cell-papillary RCC as a Distinct Histopathological and Molecular Genetic Entity.

Macroscopically, clear cell papillary renal cell carcinomas showed a variable cystic and solid morphology; some tumors exhibit a predominantly solid and white-mahogany brown appearance. The histologic features of these tumors comprise morphologic changes that are typical of both clear cell renal cell carcinoma and papillary renal cell carcinoma. Despite their diffusely papillary architecture, these tumors are entirely composed of cells with clear cytoplasm. In contrast to classic clear cell renal cell carcinoma, these tumors lack a delicate sinusoidal vascular network. Their architecture is papillary, but in contrast to classic papillary renal cell carcinomas, the tumor cells exhibit optically clear cytoplasm. Aggregates of foamy macrophages in the stroma of the papillary cores and areas of cholesterol cleft formation, findings often seen in classic type 1 papillary renal cell carcinoma, are not observed in these tumors. The differential diagnosis may be difficult, considering that clear cell renal cell carcinoma can show pseudopapillary architecture, and papillary renal cell carcinoma may exhibit components of cells with clear cytoplasm. However, pseudopapillae in clear cell renal cell carcinoma are usually only focally present, and papillary renal cell carcinomas with extensive clear changes are rare.[27,28] In the latter

the cytoplasmic clearing is typically partial with some degree of granularity remaining. Clear cell-papillary RCC show encapsulation with variable architectural patterns consisting in papillae occurring within tubules and cysts, branching tubules similar to benign prostatic acini, and tubulo-glandular structures of variable sizes and shape. Variable sized cysts can be also present, predominantly at the periphery of the tumor. All tumor cells have clear cytoplasm with nuclei aligned away from the basal membrane, resembling secretory endometrium. The nuclei of all cases are predominantly low grade (ISUP nucleolar grade 1-2), with only focal areas showing prominent nucleoli. The stroma is hyalinized although occasionally fibroleiomyomatous areas can be also seen.
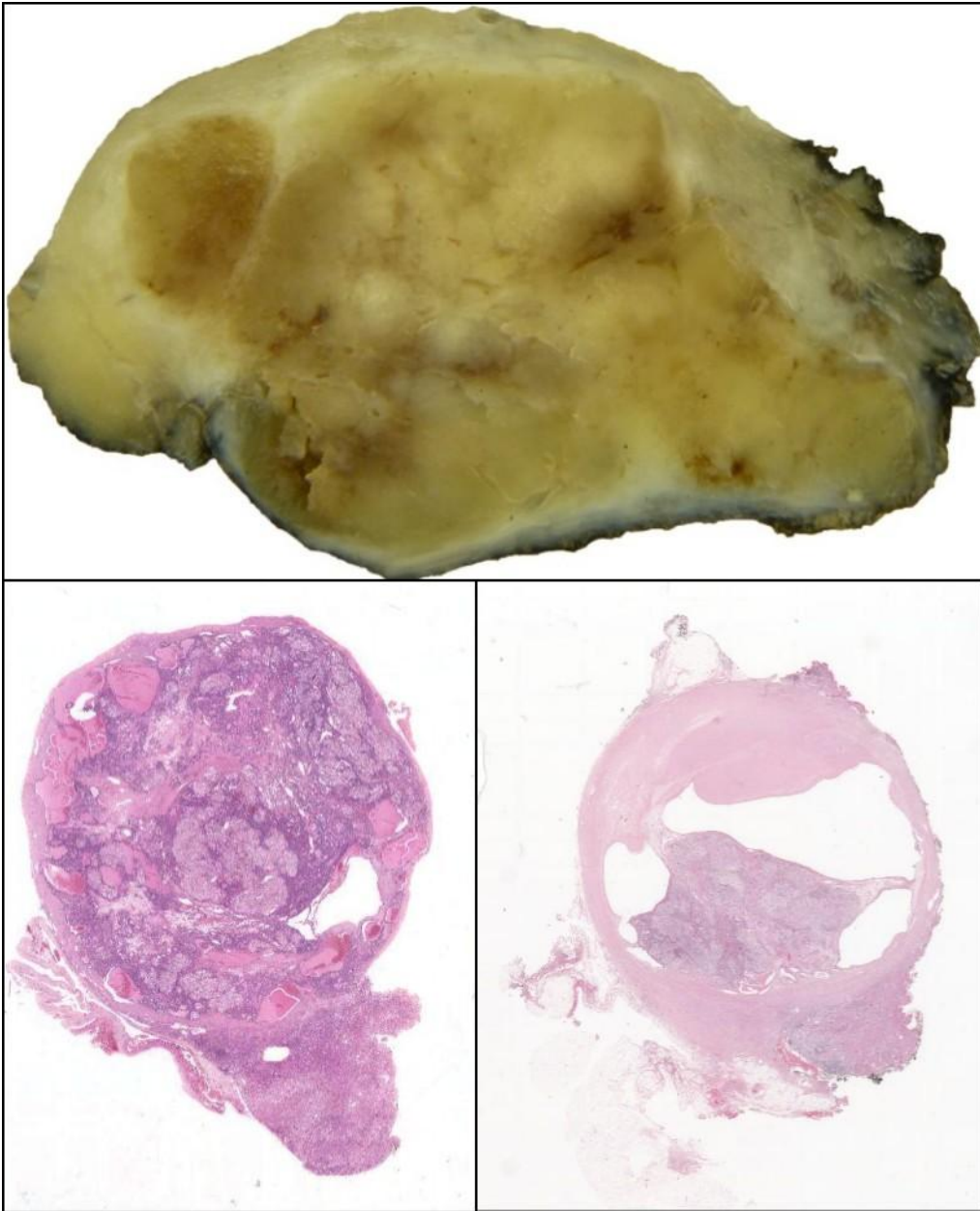
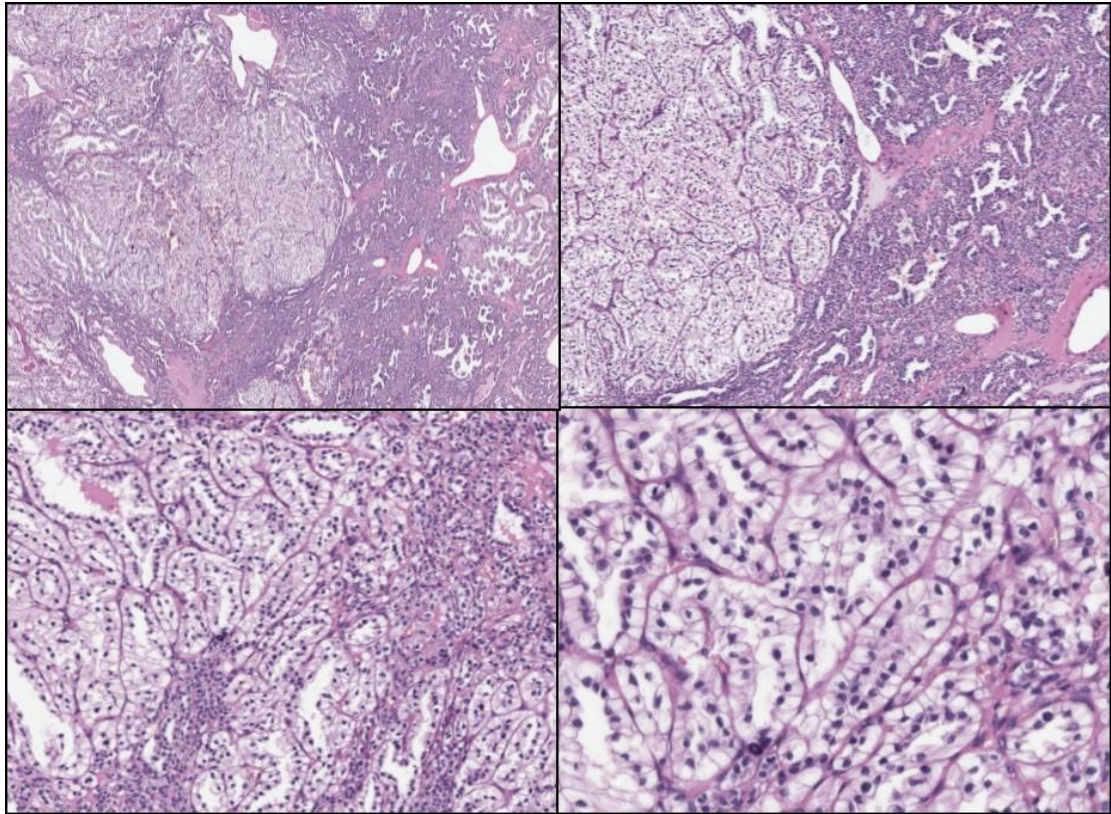**Figure 1.** Clear cell-papillary renal cell carcinoma; gross appearance.

Figure 2. Clear cell-papillary renal cell carcinoma; microscopic appearance.
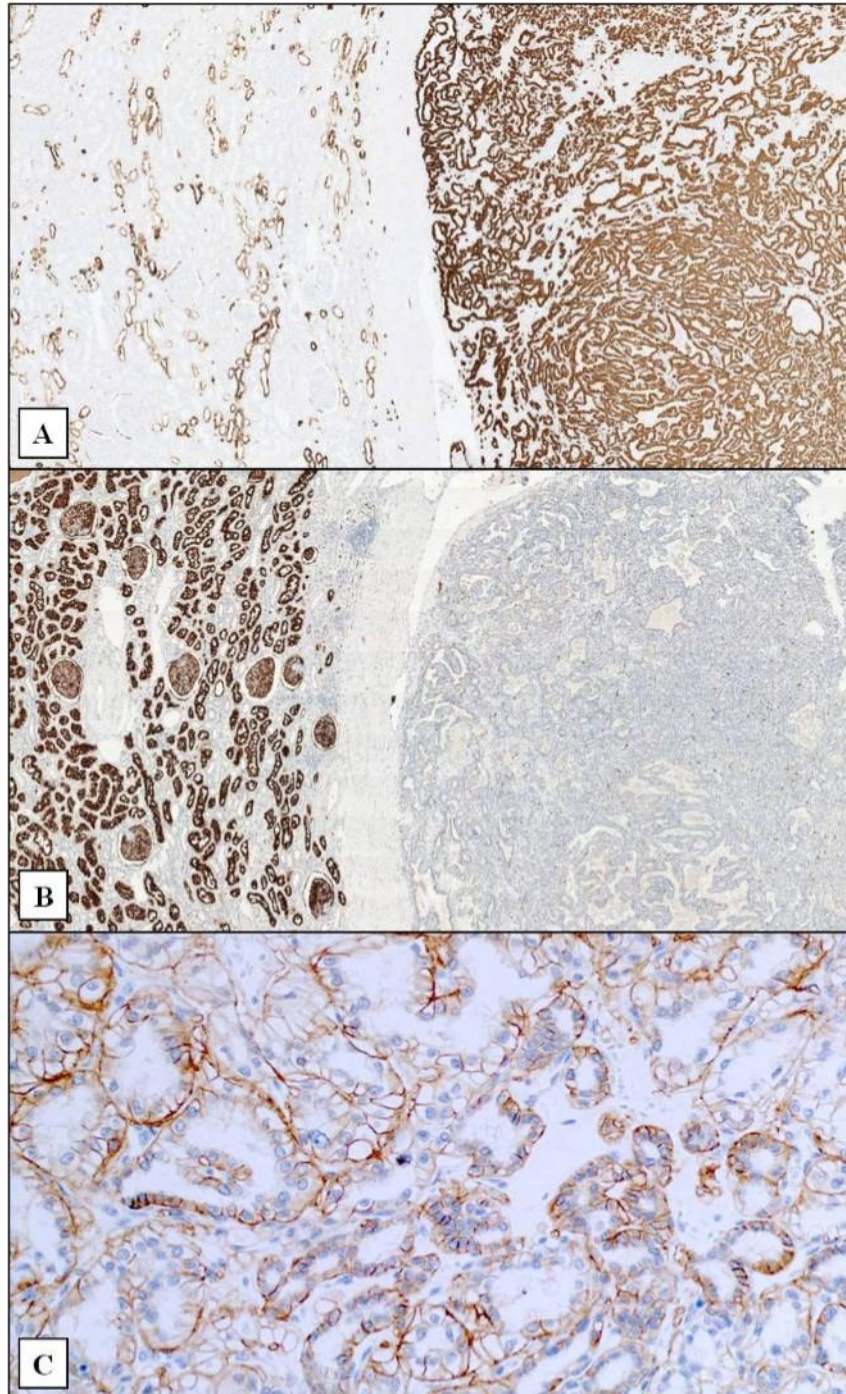
Figure 3. Clear cell-papillary renal cell carcinoma; **A:** immunoexpression of CK7; **B:** negative for CD10 (positive in the normal parenchyma); **C:** immunoexpression of CAIX.

DESIGN

The aim of my study is to better understand the molecular pattern of clear cell-papillary RCC looking for a possible specific marker that can make its diagnosis more reproducible and well distinctive from the more frequent clear cell RCC and papillary RCC.

First of all I propose a review of histological and molecular pattern of clear cell RCC and papillary RCC that are the most frequent renal cell carcinomas (80% and 15%) and that are the two entities considered in the differential diagnosis of clear cell-papillary RCC.

To validate immunohistochemical and FISH results we suggest to test sections containing also normal renal parenchyma adjacent to the neoplasia.

In normal adult kidney, CD10 stains the glomerular epithelium, Bowman's capsule and the normal proximal tubular cells, which shows a strong surface membrane staining.[29] Parvalbumin is constantly and strongly expressed, with a cytoplasmic and nuclear pattern, in a variable number of cells of distal convoluted tubules, connecting tubules, and in a subset of collecting duct cells, likely intercalated cells.[30] Strong diffuse cytoplasmic expression of cytokeratin 7 is observed within the cells of the distal tubules and collecting ducts of the non-neoplastic kidney.[31,32] Renal parenchyma displays cytoplasmic and/or a nuclear immunostaining for S100A1 in the cells lining proximal tubules, loops of Henle, collecting ducts, and Bowman's capsule.[33] AMACR immunoreactivity is present in proximal convoluted renal tubules, but very minimal to absent in distal tubules, glomeruli, medullary tubules and stromal cells.[34]

Few reports regarding FISH analysis showed the fluorescent count on normal renal parenchyma. This important issue, due probably to the procedures variability,

should be always taken as references from which statistical analysis can extrapolate standardized FISH results. It has been reported percentages of single signals, greater than 26, 27, 22, 26, and 30% for respectively chromosomes 1, 2, 6, 10, and 17 using a non-confocal microscope.[35] In normal epithelial cells in the renal tubules, nuclei with three or four centromeric signals were occasionally seen but in no sample exceeded 12% of the total. [36-38]

Clear cell renal cell carcinoma

Clear cell RCC is immmunohistochemically characterized by a high positive rate for CD10 (82%).[29,39,40] In our experience also CD13 is a good immunohistochemical marker of clear cell renal cell carcinoma being positive in 81%.[41] Expression of CD15 and S100A1 protein has been reported respectively in 75% and 73% of the cases.[33,42] Most clear cell RCCs typically shows a restricted expression pattern of cytokeratins (CK) with limited cases expressing CK8, CK19 and high weight CKs, a large portion of cases positive for CK18 and only 6% of the cases expressing CK7.[43-45] Around more than a half of clear cell RCCs reveals immunoreactivities for RCC marker, Epithelial Membrane Antigen (EMA) and vimentin.[39,40,43,46] Alpha-methylacyl-CoA racemase (AMACR) reactivity has been detected in 13 of 52 (25%) and c-kit in 1 of 40 (3%) whereas parvalbumin was found to be constantly absent.[30,34,47] Moreover, clear cell RCCs are infrequently positive for BerEP4 (27%), MOC31 (4%) and E-Cadherin (5%)[40,45,48]. Carbonic anhydrase 9 (CA9) is a protein iperexpressed in hypoxia condition and is induced through the signaling pathway involving VHL gene and HIF-alfa. The immunoexpression of CA9 is positive in clear cell RCCs and a prognostic value has been proposed.[49,50]

Membranous pattern of immunoexpression of caveolin-1 has been observed to be specific of clear cell RCC.[51]

Mutation of the Von Hippel-Lindau syndrome (VHL) gene mapping in the chromosomal region 3p25 occurs almost exclusively in this type of renal tumor. Moreover, loss of heterozygosis has been observed among 3p14, 3p21.3 and 3p25 both in sporadic and hereditary forms.[52] Probably for that reason, clear cell RCC cytogenetically shows a highly specific deletion of chromosome 3p that can be easily detected in 76% of clear cell RCCs using dual-labeling fluorescence in situ

hybridization analysis.[53] Cytogenetical studies using commercial available probes for the centromere 3 and telomere 3p, analyzing the relative depletion of 3p signals, well identify clear cell RCC.[26]

Other chromosomal aberrations observed in these tumors are copy number gains or losses of 5q21 that is thought to be events that lead to tumor progression, even if this finding has not been confirmed.[54] Loss of chromosome 14q that has been shown to have a close correlation with higher stage, higher histologic grade and poorer outcome,[55] and loss of chromosome 9p observed in 18% of clear cell RCC as an independent negative prognostic factor.[56]
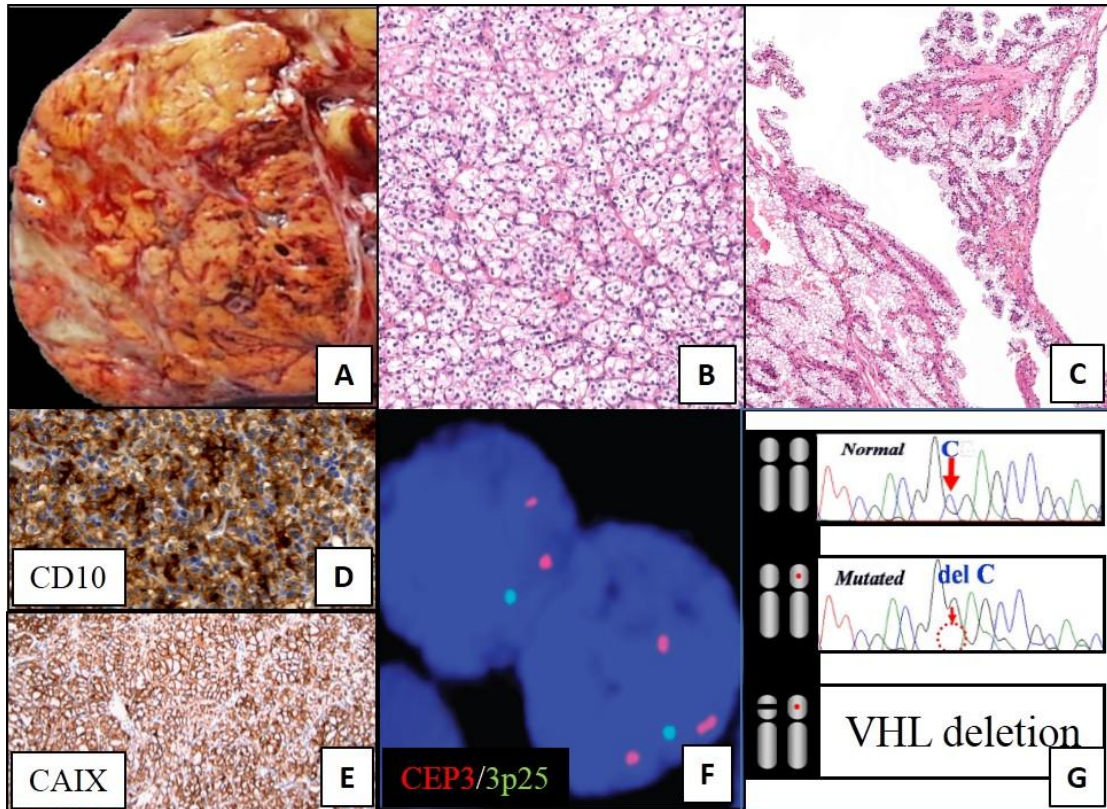
Figure 4: Clear cell renal cell carcinoma. **A:** macroscopic appearance. **B:** microscopic appearance of conventional case. **C:** pseudopapillary pattern. **D:** immunoexpression of CD10. **E:** immunoexpression of CAIX. F: FISH, deletion of 3p. **G:** molecular alteration of the gene VHL.

Papillary renal cell neoplasms

Most papillary RCCs typically express CK7 (87%), 8, 18 and 19, and vimentin (90%).[43,57] CK7 expression is more frequently observed in type 1 (87-100%) than type 2 (20-50%)[58] such as EMA (type 1 ranging from 72 to 100% and type 2 from 13 to 17%)[46,59] whereas E-cadherin is reported predominantly in type 2.[46] Both type 1 and type 2 papillary RCCs constantly show AMACR immunostain.[34,60] An high incidence of positivity for BerEP4 (67%), RCC Marker (63%)[61] and CD10 (59-90%)[29,40] is reported. S100A1 and CD15 are respectively observed in 92% and 41% of papillary RCCs[33,42] which occasionally express high molecular weight CKs (26%) and MOC31 (11%).[40]

Chromosomal aberrations occur early in the evolution of papillary renal cell neoplasia also in small tumors of a few millimeters in diameter with trisomy of chromosomes 7, 17 and loss of the Y chromosome as the most consistent genetic abnormalities. Additional chromosomal gains are observed and some authors suggest they characterize the progression from papillary adenomas to papillary RCC.[9,36,62-64] Some authors have suggested genetic differences between the two morphological types (type 1 and type 2) of papillary RCCs: type 1 cases seem to have a significantly higher frequency of allelic imbalance on 17q and type 2 cases an higher frequency of allelic imbalance on 9p.[65]

Oncocytic papillary RCC, considered a third group of papillary RCCs with a different outcome, has been reported to carry three or more signals for chromosome 7 and 17 like type 1 and type 2 papillary RCCs.[62,66]
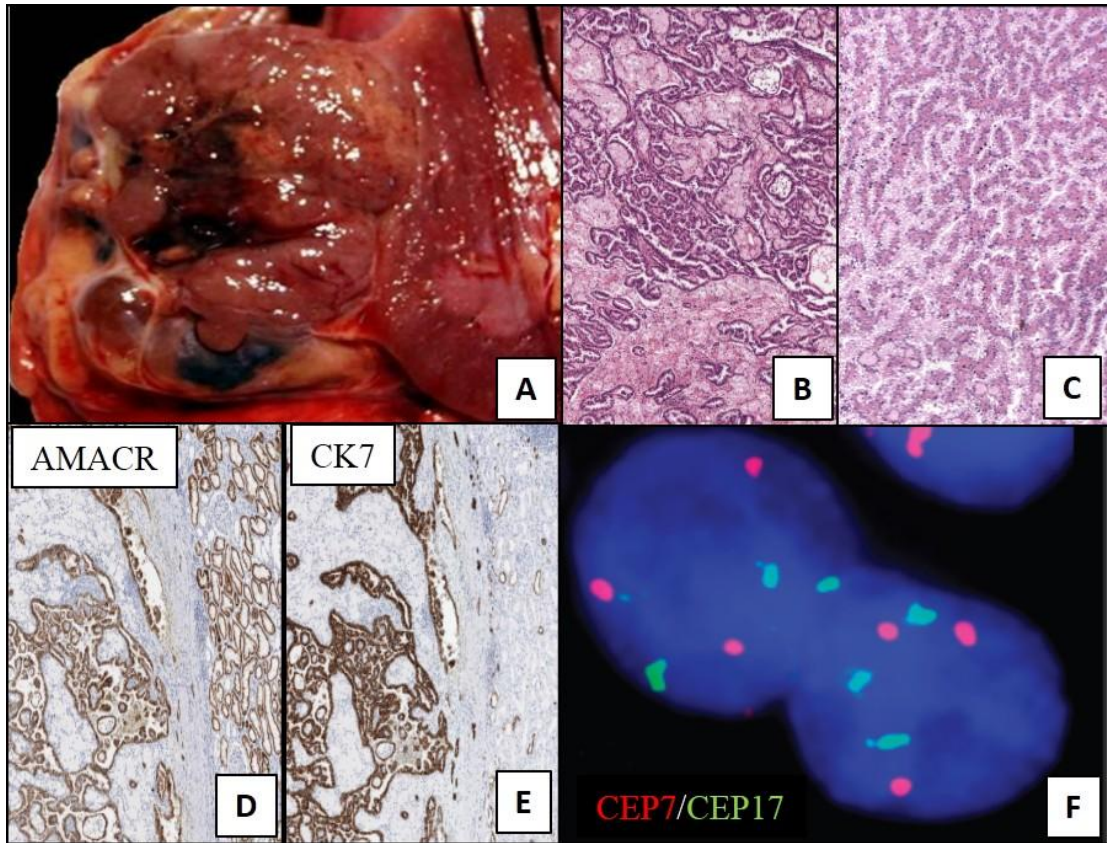
Figure 5: Papillary renal cell carcinoma. **A:** macroscopic appearance. **B:** microscopic appearance of conventional case. **C:** cytoplasmic clarification. **D:** immunoexpression of AMACR. **E:** immunoexpression of cytokeratin (CK) 7. **F:** FISH, trisomy of chromosome 7 and chromosome 17.

MATERIAL AND METHODS

Immunohistochemical Staining

Immunohistochemistry was performed with the following antibodies (summarized in table 1): cytokeratin 7 (CK7) (DAKO, Carpintera ,CA; clone OV-TL 12/30; prediluted); CD10 (Nova- castra, Burlingame, CA, USA; clone 56C6; 1:10 dilution); alpha-methylacyl-CoA racemase (AMACR) (P504S) (Dako; clone 13H7; 1:50 dilution); carbonic anhydrase IX (CAIX) (Abcam Inc, Cambridge, MA; clone ab1508; 1:1000 dilution); GATA3 (BD Pharmingen, San Diego, CA, clone L50-823, 1:50 dilution) CD10 (Nova- castra, Burlingame, CA, USA; clone 56C6; 1:10 dilution); cytokeratin 5 (Novacastra; clone XM26; 1:100 dilution); cytokeratin 34bE12 (Dako, Carpinteria, CA, USA; clone 34bE12; 1:40 dilution); cytokeratin 14 (Biogenex; clone LL002; 1:50 dilution); cytokeratin 1 (Novacastra; clone 34βB4; 1:50 dilution); cytokeratin 10 (Novacastra; clone 2HP1; 1:50 dilution); SLC2A1 (GLUT1) (Dako; polyclonal, rabbit; 1:100 dilution); vimentin (Biogenex; clone V9; 1:50 dilution); S100A1 (Dako; clone S100A1/1; 1:50 dilution); a-smooth muscle actin (Dako; clone 1A4; 1:250 dilution); HMB45 (Dako; clone HMB45; 1:300 dilution) and cathepsin K (Abcam, Cambridge, UK; clone 3F9; 1:2000 dilution). Briefly, slides were deparaffinized twice in xylene for 5 min and rehydrated through graded ethanol solutions to distilled water. Antigen retrieval was performed by heating sections in citrate buffer, EDTA buffer, or enzymatically with proteinase K. Inactivation of endogenous peroxidase activity was obtained by incubating sections in 3% H_2O_2 for 15 min. Localization of bound antibodies was performed with peroxidaselabeled streptavidin–biotin system (DAKO, LSAB2 Kit) with 3,3'-diaminobenzidine as a chromogen. Appropriate positive controls for each antibody were run concurrently and showed adequate immunostaining. Normal renal

parenchyma adjacent to the tumors was used as a control. A total of 442 cases of conventional clear cell renal cell carcinoma were used as control for our immunohistochemical analysis: 180 cases as whole sections and the remaining 262 distributed on 8 tissue microarrays including 221 primary carcinomas and 41 metastatic carcinomas.

Antigen		Clone		Dilution		Company
CK7		OV-TL12/30		1:500		Biogenex, Fremont, CA, USA
CD10		56C6		1:10		Novacastra, Burlingame, CA, USA
AMACR		13H7		1:25		Dako, Carpinteria, CA, USA
CAIX		Policlonale		1:1000		Abcam, Cambridge, UK
SLC2A1 (GLUT1)		Policlonale		1:100		Dako, Carpinteria, CA, USA
34βE12		34βE12		1:40		Dako, Carpinteria, CA, USA
CK14		LL002		1:50		Biogenex, Fremont, CA, USA
CK5		XM26		1:100		Novacastra, Burlingame, CA, USA
CK1		34βB4		1:50		Novacastra, Burlingame, CA, USA
CK10		2HP1		1:50		Novacastra, Burlingame, CA, USA
GATA3		L50-823		1:150		BD Pharmingen, San Diego, CA, USA
S100A1		S100A1/1		1:50		Dako, Carpinteria, CA, USA
HMB45		HMB45		1:300		Dako, Carpinteria, CA, USA
Catepsina K		3F9		1:2000		Abcam, Cambridge, UK
Vimentina		V9		1:50		Biogenex, Fremont, CA, USA
Actin SM		1A4		1:250		Dako, Carpinteria, CA, USA

Table 1: Antigens used for the immunohistochemical analyses.

Fluorescence In Situ Hybridization

Series of 4 μm slides were prepared from buffered formalin fixed, paraffin embedded tissue blocks. The slides were deparaffinized with two washes of xylene, 15 min each, and subsequently washed twice with absolute ethanol, 10 min each and then air dried in the hood. Next, the slides were treated with 0.1mM citric acid (pH 6.0) (Zymed, CA, USA) at 95°C for 10 min, rinsed in distilled water for 3 min followed by a wash of 2×SSC (standard saline citrate) for 5 min. Digestion of the tissue was performed by applying 0.4 ml of pepsin (5 mg/ml in 0.1N Hcl/0.9 NaCl) (Sigma, St Louis, MO, USA) at 37°C for 40 min. The slides were rinsed with distilled water for 3 min, washed with 2×SSC for 5 min and air dried. FISH was performed with centromeric α-satellite DNA probes for chromosome 7 (CEP 7, Spectrum Green), 17 (CEP 17, Spectrum Orange), Y (CEP Y, Spectrum Green), 3 (CEP3, Spectrum Orange) and subtelomeric probe for 3p25 (3pTel25, Spectrum Green). All of the probes were from Vysis (Downers Grove, IL, USA) and were diluted with *tDenHyb*1 (CEP 7-CEP 17 and CEP Y) and *tDenHyb* 2 (CEP 3-3pTel25) (Insitus, Alburquerque, NM, USA) in a ratio of 1:100, respectively. 5 μl of diluted probe was applied to each slide in reduced light conditions. The slides were then covered with a 22×22mm cover slip and sealed with rubber cement. Denaturation was achieved by incubating the slides at 83°C for 12 min in a humidified box and hybridization at 37°C overnight. The cover slips were removed and the slides were washed twice with 0.1XSSC/1.5M urea at 45°C (20 min for each), followed by a wash with 2×SSC for 20 min and with 2×SSC/0.1% NP-40 for 10 min at 45°C. The slides were further washed with room temperature 2×SSC for 5 min. The slides were air dried and counterstained with 10 μl DAPI (Insitus, Albuquerque, NM, USA), covered with cover slips and sealed with nail polish.[38,67,68]The slides were examined using a Zeiss

Axioplan 2 microscope (ZEISS, Gottingen, Germany) with the following filters from

Chroma (Chroma, Brattleboro, VT, USA): SP-100 DAPI, FITC MF-101 for Spectrum

Green (CEP 7, Y and 3pTel25) and Gold 31003 for Spectrum Orange (CEP 3 and 17).

The images were acquired with a CCD camera and analyzed with MetaSystem Isis

Software (MetaSystem, Belmont, MA, USA). Five sequential focus stacks with 0.4

mm intervals were acquired and then integrated into a single image in order to reduce

thickness-related artifacts.

We performed fluorescence in situ hybridization analysis with the same

probes (CEP 7, 17, 3 and 3pTel25) in classic clear cell renal cell carcinoma and

classic papillary renal cell carcinoma as controls.

In Situ Hybridization Analysis

The method of analysis was partially described previously.[9,35,69,70] In brief, for

each slide, 100 to 150 nuclei from tumor tissue were scored for signals from probes

under the fluorescence microscope with ×1000 magnification. Non-neoplastic kidney

parenchyma was used as control. Definitions of chromosomal gain and loss of

chromosomes 7, 17 and Y were based on the Gaussian model and related to the non-

neoplastic controls. Any tumor with the signal score beyond the cutoff value was

considered to have gain or loss of specific chromosome. The cutoff values for each

probe were set at mean plus three standard deviations (S.D.) of the control values.

Statistical method to analyze 3p deletion was referred to previous studies on deletion

of chromosome 1p and 19q in oligodendrogliomas.[71] The cutoff value for the 3/3p

ratio was set at mean plus three standard deviations (S.D.) of the 3/3p ratio in non-

neoplastic cells. Any tumor with 3/3p ratio beyond the cutoff values was considered

to have deletion of 3p25.

Array Comparative Genomic Hybridization and Data Analysis

Microdissection from the three formalin-fixed paraffin-embedded kidney tumors was performed manually, with accurate attention in obtaining material from the epithelial zones of tissue slides.

Genomic DNA was isolated using the QIAamp DNA mini kit (Qiagen Nordic, Finland) and quanti- fied on the NanoDrop spectrophotometer (NanoDrop Technologies Inc, DE, USA). As a reference, we used DNA from pooled peripheral blood leukocytes of healthy males. Using the Agilent Human 244K array format containing B240 000 oligonucleotide probes, covering both coding and non-coding genome re- gions (Agilent Technologies, Santa Clara, CA, USA), we screened copy number alterations in all three tumors. Briefly, 1.5mg of tumor and reference DNA were digested, labelled, and hybridized according to the Agilent protocols. The array images obtained after scanning (Agilent scanner G2565BA) were processed with the Feature Extraction software (version 10.5), and the output data files were analyzed with the Agilent Genomic Workbench. To identify copy number alterations, we used aberration detection method 2 (ADM-2) algorithm and to exclude the small variances in the data, we set up a custom aberration filter identifying alterations in copy number if a minimum of eight probes gained or lost were identified and with a minimum absolute average log ratio for the region being 0.5. Regions with small copy number variations were excluded by comparing and visualizing the copy number variant regions tool of the Genomic Workbench software.

ch fluorescent score number.

***VHL* sequencing analysis**

Five 10-μm thick sections of tumor tissue were cut from formalin-fixed

paraffin-embedded blocks. Epithelial and smooth muscle components were separated

by manual microdissection. DNA was extracted separately from each component.

Polymerase chain reaction (PCR) for *VHL* gene analysis was performed using primer

sequences as reported.[72,73] Normal tissues from the same patients were used as a

reference. The reaction conditions were as follows: 12.5 μl of HotStart Taq PCR

Master Mix (QIAgen, Hilden, Germany), 10 pmol of each primer, 100 ng of template

DNA, and distilled water up to 25 μl. Amplification program for all fragments, except

the marker D3S666, consisted of denaturation at 95°C for 15 min, then 40 cycles of

denaturation at 95°C for 1 min, annealing at 55°C for 1 min, and extension at 72°C

for 1 min. The program was finished by 72°C incubation for 7 min. Annealing

temperature for fragment D3S666 was 58°C. PCR products of the *VHL* gene were

purified with Montage PCR Centrifugal Filter Devices (Millipore, Billerica, MA,

USA) and sequenced using a Big Dye Terminator Sequencing kit (PE/Applied

Biosystems, Foster City, CA, USA). Samples were then run on an automated

sequencer ABI Prism 310 (PE/Applied Biosystems) at a constant voltage of 11.3 kV

for 20 min. PCR products of STR markers were mixed with a size marker and run on

an automated sequencer ABI Prism 310 (PE/Applied Biosystems) at a constant

voltage of 15 kV for 28 min. Genomic DNA was isolated from three 5μM- thick

paraffin sections of each renal carcinoma sample using the Ex-Wax DNA Extraction

Kit (Chemicon International, Temecula, CA, USA) according to manufacturer

instructions. Bidirectional sequencing of PCR products was performed by using a

ABI PRISM BigDye terminators v3.1 cycle sequencing kit (Applied Biosystems,

Foster City, CA, USA), and sequences were run on an Applied Biosystems 3130

Genetic Analyzer (Applied Biosystems) and compared with the reference sequence

CCDS 2597.1. The PCR amplicon carrying the mutation was subcloned into a

pGEM®-T Easy vector (Promega, Madison, WI), transformed in competent DH5α

cells and plated onto LB agar with ampicillin and X-gal selection. Then, 12 distinct

blank (white) colonies were chosen, plasmid DNA was extracted and submitted for

amplification and sequencing of *VHL* exon 3 as described above.

Methylation-specific multiplex ligation-dependent probe amplification (MS–MLPA)

and CpG methylation analysis

Microdissection of tissues from formalin-fixed paraffin-embedded kidney tumors was

performed manually. Genomic DNA extracted from the three samples was subjected

to MS-MLPA using ME001-0808-C1 and ME002-0809-B1 probemixes (MRC-

Holland, Amsterdam, The Netherlands) with 20-100 ng of DNA per sample. The

standard MS-MLPA-protocol was employed.[74] Both probemixes contained one

specific MLPA probe for the exon 1 of *VHL* gene that has a recognition site for a CpG

methylation-sensitive endonuclease HhaI. The MS-MLPA product fragments were

analyzed by a ABI model 3130 capillary sequencer (Applied Biosystems,

Nieuwerkerk aan den Ijssel, the Netherlands) using Genescan-ROX 500 size

standards. As the same probemixes are intended to detect both copy number and

methylation changes of the target genes simultaneously, both methylation and copy

number status was analysed using Coffalyser software (MRC-Holland, Amsterdam,

The Netherlands)[75]. The data were first normalized by dividing the peak area of a

single probe by a cumulative peak area of all control probes (not degraded by HhaI).

Then, the normalized peaks from the HhaI digestion reaction were compared to the

normalized peaks from the undigested control reaction. Final methylation value for

each sample was obtained by subtracting the background methylation values of the control samples (male and female DNA samples, Promega, WI, USA). The following criteria were used for determining the methylation status: 0.00-0.25 (absent), 0.25-0.50 (mild), 0.50-0.75 (moderate), and > 0.75 (extensive methylation). For copy number analysis the following cut-off values were used: <0.7 and >1.3 gain. One DNA sample (labelled 8656) was excluded from the analysis due to the low amount of DNA and for another sample (labelled 10684) we were able to include only results using ME002-0809-B1 probemix as no DNA was available for the further analysis using the ME-001-0808 mix.

RNA extraction

In each case, a representative formalin fixed paraffin embedded (FFPE) tissue sample was chosen for RNA extraction. Ten unstained slides 8μm thick were cut from blocks and a sterile scalpel was used to microdissect tumor cells (80 % or more) after deparaffinization with xylene and ethanol washing. Total RNA was extracted using the RecoverAll Total Nucleic Acid Isolation (Ambion Inc., Austin, TX, USA) according to manufacturer's protocol. RNA quantity was measured by using NanoDrop Spectrophotometer ND-1000. RNA quality was evaluated using Bioanalyzer 2100 (Agilent Technologies, Santa Clara, CA).

Microarray hybridization

Four matched tumor and normal samples constituted our discovery set and were submitted for microarray analysis. This was performed using the Human miRNA Microarray Kit Release 16.0, 8x60K (G4870A, Agilent Technologies, Santa Clara, CA) according to manufacturer's protocols. The array contains 1205 human

microRNAs from the Sanger database v16.0
(http://microrna.sanger.ac.uk/sequences/). Only samples with 28S/18S>1.2, RIN>8
and detectable miRNA were used for the analysis.

Microarray hybridization was performed at Sidney Kimmel Cancer Center Microarray
Core Facility at Johns Hopkins University using manufacture's instruction as
previously described[76]. Data were acquired with Agilent Feature Extraction 9.5.3.1
software for miRNA microarray. Two data files are generated for each array: Feature
Extraction file contains signal intensities from all individual probes and GeneView
file contains summarized signal intensities for each miRNA by combining intensities
of replicate probes and background subtraction.

Technical validation of microarray data

Individual TaqMan microRNA assays (Applied Biosystems, Austin, TX) were used
for validation of microarray findings in the above discovery set of 4 cases as well as
11 additional cases (validations set). The individual miRNAs were selected among the
miRNAs that showed to be the most differentially expressed in the microarray
experiments. RNU6B was used as reference gene for normalization. Total RNA (10
ng) was reverse transcribed using TaqMan MicroRNA Reverse Transcription Kit
(Applied Biosystems, Austin, TX). qRT-PCR was performed using TaqMan
Universal Master Mix II (Applied Biosystems, Austin, TX) on a 7900HT Fast Real
Time PCR System according to the manufacturer's protocol. All samples were run in
triplicate. Normalized signal levels for each miRNA were calculated using
comparative cycle threshold method ($\Delta\Delta$CT method)[77].

Statistical Analysis

MicroRNA expression data was processed for statistical analysis using packages from R/Bioconductor (www.bioconductor.org) as previously described [78-80]. Briefly, a generalized linear model was fit for each miRNA to estimate expression differences between clear cell papillary tumor and normal kidney, and an empirical Bayesian approach was employed to moderate standard errors of expression fold-change. Multiple testing corrections were performed using the Benjamini-Hochberg method. In order to identify consensus of differentially regulated miRNA between renal carcinoma histologic types, we additionally determined differential miRNA expression using two publically available microarray datasets from the NCBI Gene Expression Omnibus (GEO) database (GSE41282 and GSE3798). In these two datasets we identified the miRNA expression profiles that distinguish the different tumor groups from normal counterparts. The meta-analysis was performed by comparing the lists of differentially expressed miRNA between the groups of interest independently obtained from each analyzed dataset with a false discovery rate of 5% or less. We also performed comparisons between pairs of data sets using Correspondence At the Top plots (CAT-plots), and evaluated the number of concordant overlapping genes using Venn diagrams. CAT-plot confidence intervals and probabilities of observing the identified number of concordant overlapping genes in the Venn diagrams by chance alone were based on the hyper-geometric distribution, as previously described[78-80].

RESULTS

Immunohistochemical findings

GATA3 was expressed by 7/13 (54%) clear cell papillary renal cell carcinomas. Cases that stained positive for GATA3 showed expression of the marker in a percentage of cells variable from 10% to 90% (mean 47%). All cases showed a diffuse positivity for cytokeratin 7 in 70-100% of cells. CK AE1-AE3 expression was seen in 100% of the neoplastic cells in all cases. SLC2A1 (GLUT1) and CAIX displayed variable intensity of expression in all and in all but one case, respectively. Cytokeratin 34βE12 and CK14 showed an equivalent pattern of staining as they were expressed in the same 12 cases (12/14, 86%). CK1 and CK10 were constantly negative while CK5 showed positivity in 4 cases. Alpha-methylacyl-CoA racemase (P504S), HMB-45, cathepsin k, androgen receptor, and estrogen and progesterone receptors were constantly negative. S100A1 was expressed in 9/13 cases (1 case was not available), while parvalbumin showed weak immunoreactivity in 10% of the neoplastic cells in one case.

The stroma of the tumors showed focal positivity for alpha-smooth muscle actin in 12/14 cases (85%).

Only 2/150 CCRCC cases (1%) of the TMAs stained weakly positive for 34βE12 and CK14.

We previously stained the same 150 conventional clear cell renal cell carcinomas for CK7 and found it positive in 36/150 (24%) of the cases.

In our cohort of conventional clear cell renal cell carcinomas GATA3 positivity was seen in only 1/292 (0,3%) of cases that included whole slides of 180 primary carcinomas and TMA spots of 71 primary 41 metastatic carcinomas.

n.	CK7	CD10	AMACR	CAIX	GLUT-1	S100A1	HMB45	CAT K	VIM	ACT SM	34βE12	CK14	CK5	CK1	CK10	GATA3
1	80	neg	neg	50	50	neg	neg	neg	neg	60	60	30	neg	neg	neg	neg
2	100	10	neg	60	30	neg	neg	n.a.	neg	70	100	60	80	neg	neg	neg
3	70	70	neg	10	80	10	neg	neg	neg	10	neg	neg	neg	neg	neg	neg
4	80	neg	neg	90	90	30	n.a.	neg	neg	30	20	40	neg	neg	neg	neg
5	90	40	neg	40	40	50	neg	neg	neg	60	80	40	30	neg	neg	60
6	80	neg	neg	30	50	neg	neg	n.a.	neg	10	neg	neg	neg	neg	neg	neg
7	100	neg	neg	50	70	n.a.	neg	n.a.	70	30	80	60	neg	neg	neg	40
8	100	neg	neg	n.a.	n.a.	60	neg	neg	n.a.	neg	80	80	neg	neg	neg	80
9	90	neg	neg	30	70	neg	neg	neg	neg	neg	30	30	neg	neg	neg	60
10	90	neg	neg	60	90	10	neg	neg	neg	30	60	20	neg	neg	neg	30
11	90	10	neg	90	70	70	neg	neg	neg	70	90	60	10	neg	neg	10
12	70	40	neg	90	60	60	neg	neg	20	80	80	70	neg	neg	neg	neg
13	80	50	neg	90	60	90	n.a.	neg	neg	40	80	50	10	neg	neg	10
14	70	10	neg	90	50.	80	n.a.	neg	neg	70	30	20	neg	neg	neg	neg

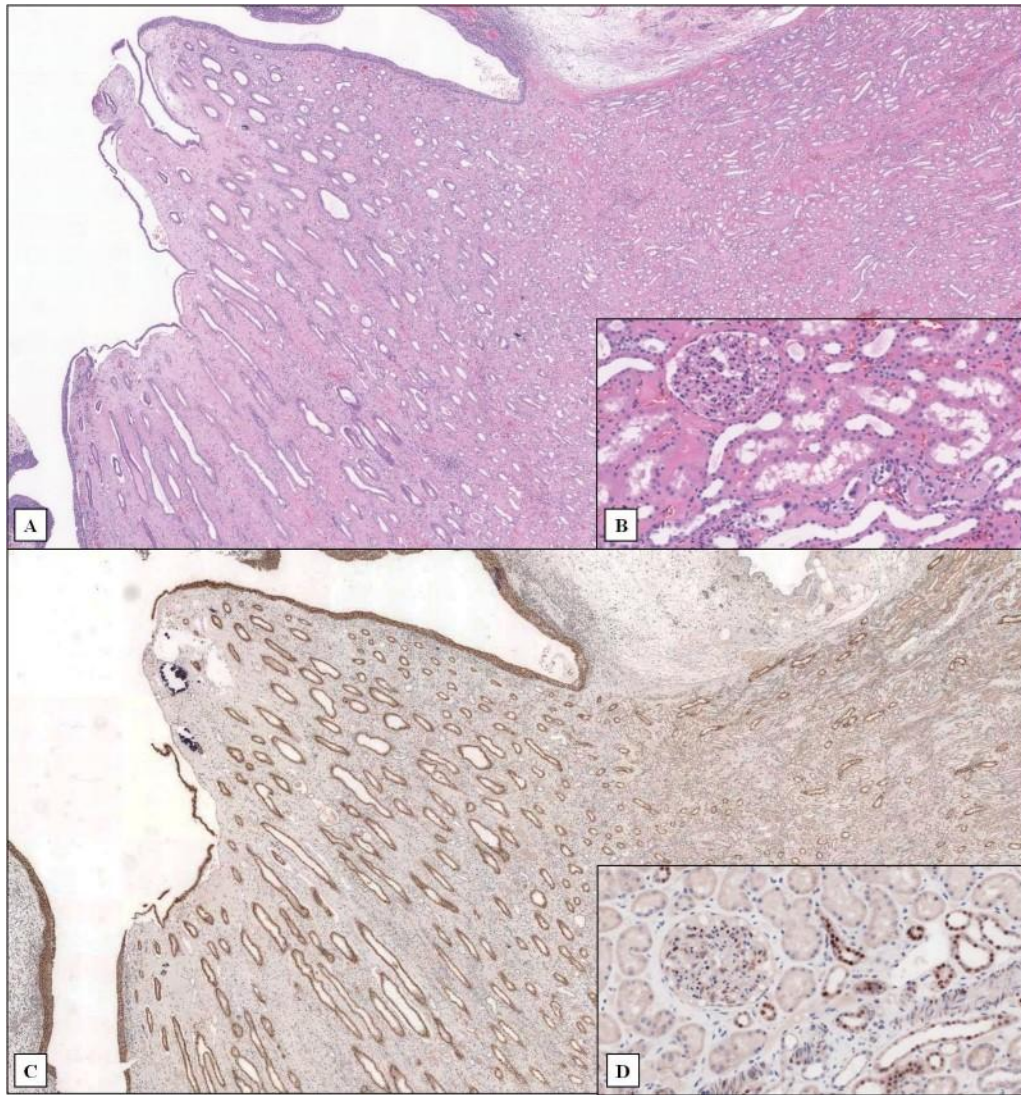**Table 2:** Immunohistochemical results.

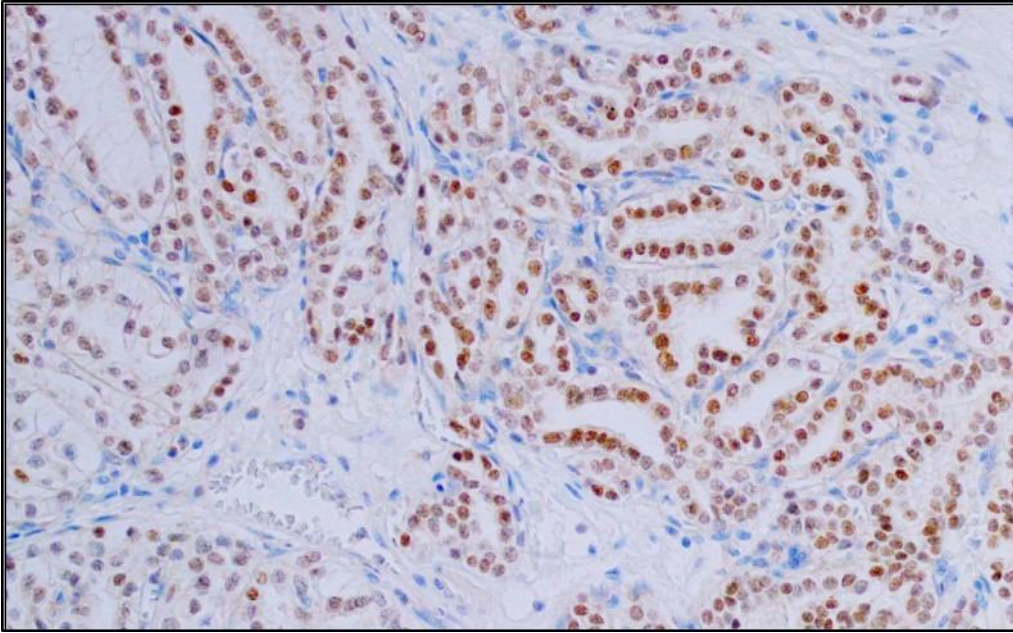**Figure 6.** Pattern of immunoexpression of GATA3 in normal parenchyma.

Figure 7. Nuclear immunoexpression of GATA3 in clear cell-papillary renal cell carcinoma.
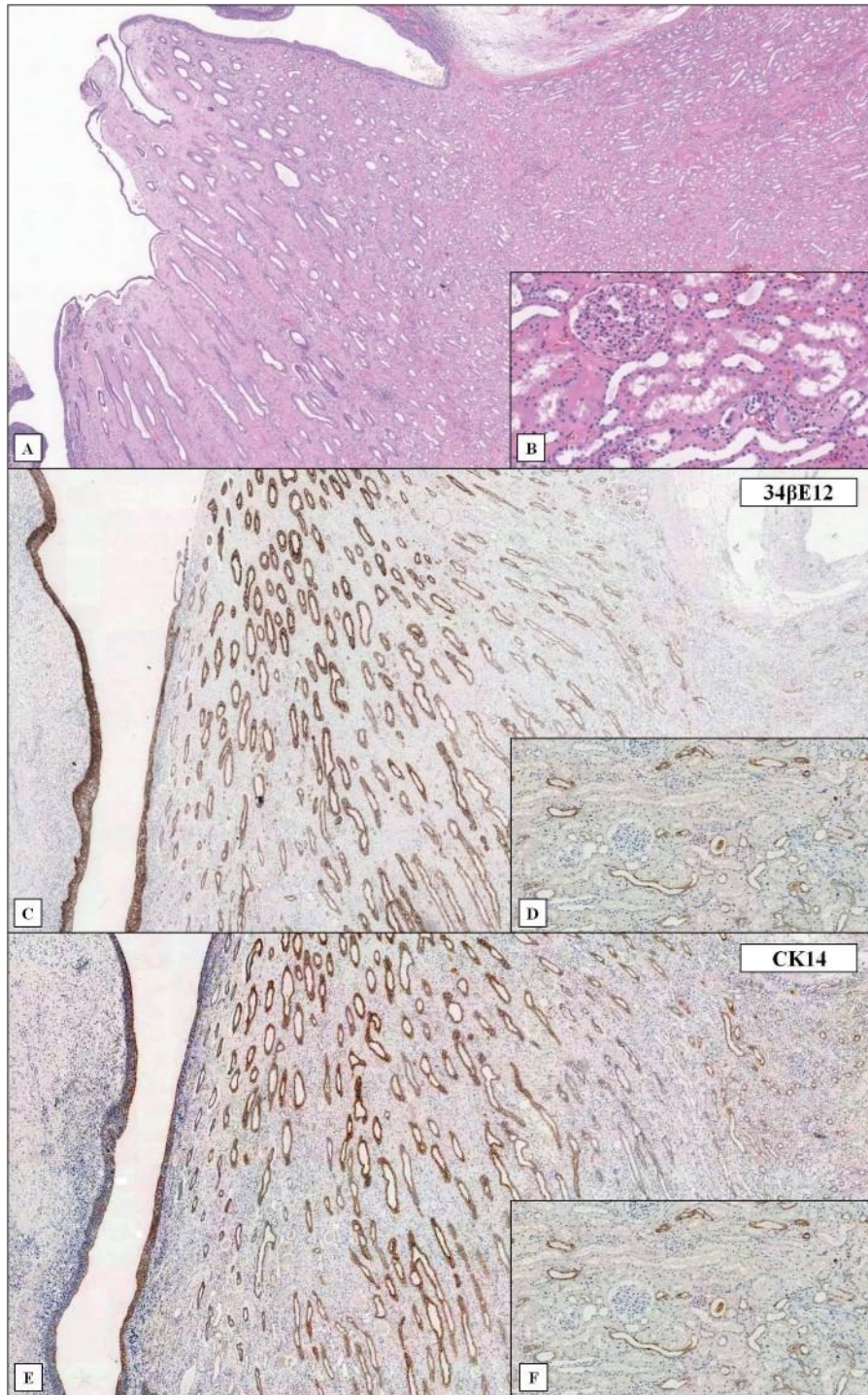
Figure 8. Pattern of immunoexpression of 34βE12 and CK14 in normal renal parenchyma.
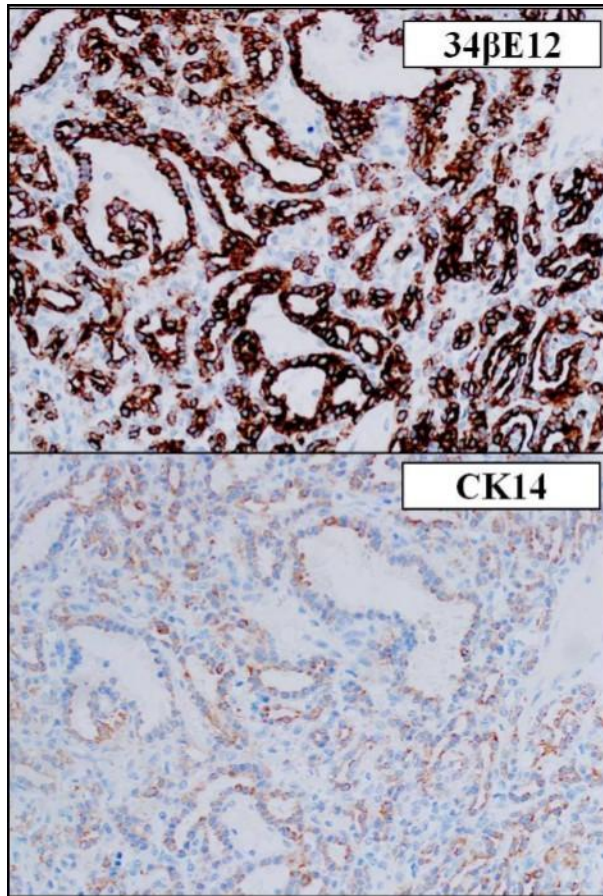
Figure 9. Immunoexpression of 34βE12 and CK14 in clear cell-papillary renal cell carcinoma.

Array Comparative Genomic Hybridization Findings

Array comparative genomic hybridization was performed in 4 cases of clear cell papillary renal cell carcinoma. We did not observe any gene copy number abnormalities. A flat profile was observed in each tumor.
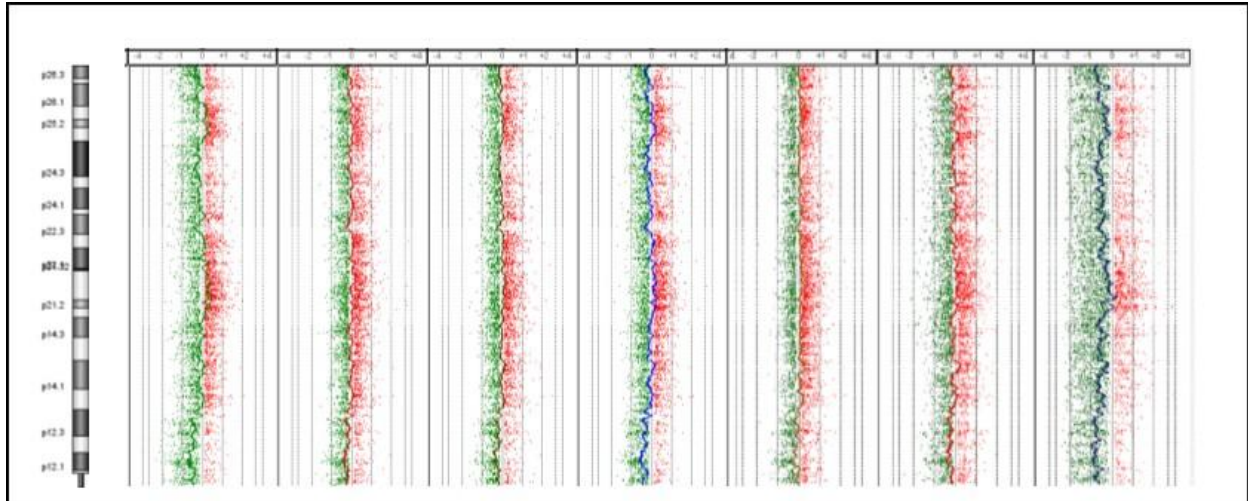

Figure 10: CGH results. Chromosome 3, flat profile.

Fluorescence in situ hybridization (FISH) findings

Locus specific sub-telomeric 3p probe: For clear cell papillary renal cell carcinomas, the average of the cases showed single, double and three or more fluorescent signals respectively in of 31%, 62% and 7% of neoplastic epithelial nuclei.

Centromeric chromosome 3 probe: For clear cell papillary renal cell carcinomas, the aberage of cases showed single, double and three or more fluorescent signals respectively in 28%, 63% and 9% of neoplastic epithelial nuclei. The value of the ratio of the normal renal parenchyma+3SD set to 1,03+3SD0,05= 1,19. In clear cell papillary renal cell carcinomas, the mean ratio was 1,06 (not deleted).

All clear cell papillary renal cell carcinoma tumours showed no gains of chromosomes 7 and 17 with single signals ranging from 33 to 43, double signals from 53 to 61 and more than two signals from 5 to 15, respectively.
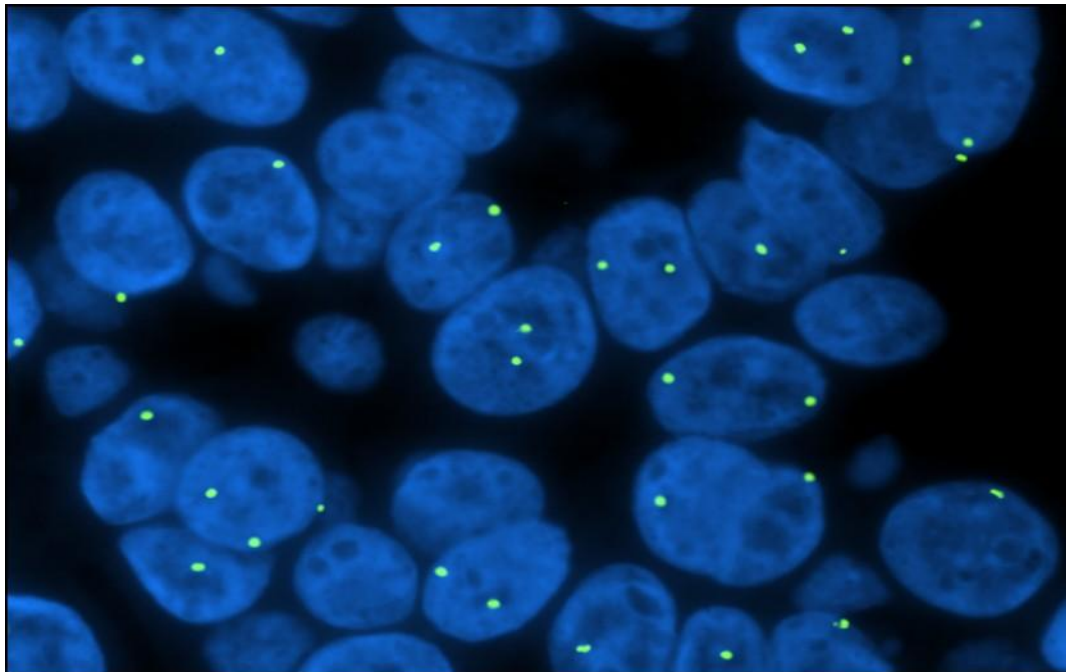

Figure 11. FISH: disomic pattern of 3p25.

VHL gene mutation

No mutation of coding sequence of the *VHL* gene was found in epithelial neoplastic components in all the clear cell papillary renal cell carcinomas tested.

MLPA findings on methylation and copy number status of VHL

We performed methylation-specific ligation-dependent probe amplification analysis in 4 clear cell papillary renal cell carcinomas. MS-MLPA analysis of FFPE tissue DNA samples showed absent or mild methylation of *VHL* gene in all cases.

Genome wide microRNA expression profiling of clear cell papillary renal cell carcinoma

Among the 1,205 miRNAs contained in the microarray, 342 mature miRNA were differentially expressed between CCPRCC and normal samples with a false discovery rate (FDR) of < 10% (supplementary table S1). Table 2 shows the most significantly differentially expressed (FDR <5%) miRNAs in CCPRCC compared to matched normal renal parenchyma.

To identify differentially expressed miRNA between CCPRCC, CCRCC and PRCC we analyzed the GSE41282 dataset, containing the expression profile of 6 CCRCC and 14 PRCC samples with corresponding normal tissue in order to derive miRNA gene expression profiles associated with CCRCC and PRCC compared to normal kidney. We respectively identified 16 and 2 microRNA moieties as differentially expressed (Supplementary Table S2a and S2b). We further analyzed the GSE37989 dataset, containing microarray-based profiles of 9 metastatic CCRCC and 12 primary CCRCC with corresponding non malignant tissue to identify the miRNA profiles associated with primary and metastatic clear cell renal carcinoma[81]; we

identified 53 and 20 differentially expressed miRNA, respectively (Supplementary Table S3a and S3b). We finally compared our data from CCPRCC to the above datasets. Because the publically available datasets were derived from different platforms with lower numbers of unique mature miRNA, we performed this cross platform comparison using differentially expressed miRNA at a higher significance threshold (FDR of 5%). In particular we compared gene expression profiles distinguishing CCPRCC, CCRCC and PRCC from normal samples by CAT-plots and Venn diagram, using the results from our profiling and the analysis of the GSE41282 dataset. This comparison revealed that at the molecular level CCPRCC more closely resembled CCRCC (figure 2 and table 3). We used a similar approach to compare our CCPRCC findings with miRNA profiles of primary and metastatic CCRCC. This latter analysis showed that at the miRNA level CCPRCC more closely resembled primary CCRCC.

Technical validation of microarray findings

Among the most differentially expressed miRNAs in the microarray experiments, miR-122, miR-135a and miR-204 were used for technical validation using qRT-PCR. The expression levels of these miRNAs was assessed in all 15 CCPRCC samples, including the initial 4 cases that were used for microarray experiments. All samples had matched normal renal tissue. Our qRT-PCR results were in agreement with the microarray findings, validating the robustness of microarray analysis.
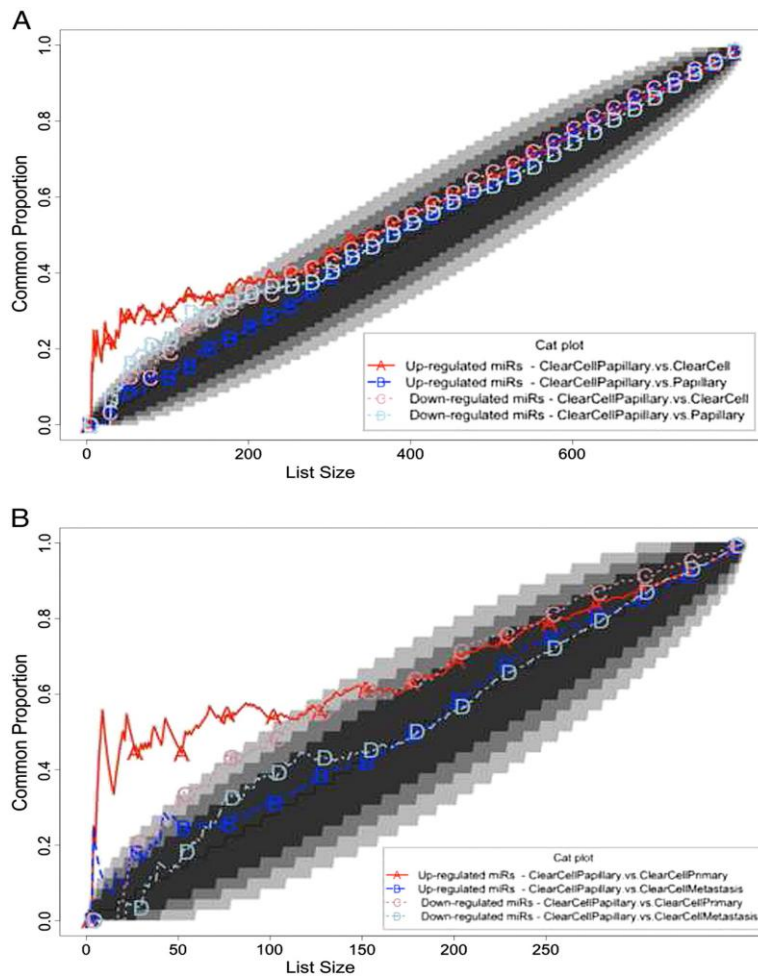
Figure 12: Consensus among miRNA profiles associated with distinct renal carcinoma histotypes and stages. Lines above the 45° diagonal lines correspond to comparisons having more agreement than would be expected by chance. Lines in the white area of the graph have a probability of agreeing by chance of less than 1E-06. Geneswere ranked by t-statistic as obtained fromthe linearmodel analysis. **A:** CAT curves for the following comparisons: miRNA up-regulated and down-regulated in clear cell papillary and clear cell tumors; miRNA up-regulated and down-regulated in papillary and clear cell papillary tumors. **B:** CAT curves for the following comparisons: miRNA up-regulated and down-regulated in clear cell papillary and in primary clear cell tumors; miRNA up-regulated and down-regulated in clear cell papillary and clear cells tumor metastasis.
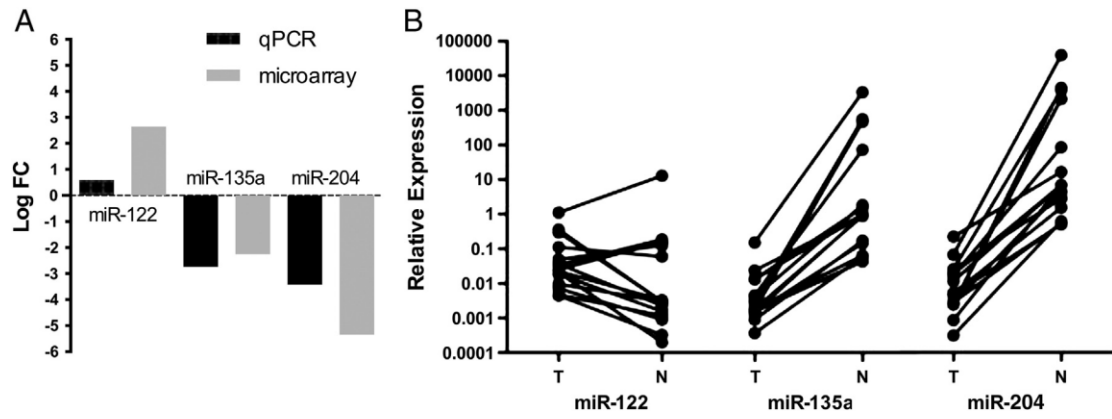
Figure 13. Technical and independent set validation of miR-122, miR-135a, and miR-204. **A:** Average fold changes of samples used for the microarray experiments and qRT-PCR experiments. **B:** Relative expression on the 3 miRNAs in all 15 cases.

miRNA Name	logFC	P Value	FDR	Proposed function	Selected validated targets
miR-210	4.26	4.46E-04	5.38E-04	hypoxamir	ISCU, HIF1A, MNT
miR-34a	2.75	1.06E-02	2.01E-03	oncosuppressor	AKT1, PTEN, c-MYC
miR-122	2.64	1.79E-04	8.96E-03	oncosuppressor	CDKN2D, SMARCD1, CCND1
miR-21	2.47	4.06E-02	5.43E-03	oncogene	PTEN, TIMP3, PDCD4
miR-34b*	2.20	3.81E-03	1.15E-03	oncosuppressor	VEGFA, CREB1, c-MYC
miR-489	2.16	2.26E-03	2.50E-02	oncosuppressor	SRC, COMP, GHRHR
miR-4284	-2.07	9.74E-04	5.87E-04	-	-
miR-1202	-2.18	2.65E-04	1.06E-02	-	-
miR-135a	-2.24	2.22E-04	1.03E-02	oncosuppressor	APC, JAK2, FLAP
miR-1973	-2.61	2.11E-03	2.44E-02	-	-
miR-204	-5.34	2.87E-04	1.06E-02	oncosuppressor	VEGFA, RUNX2, E2F3

Table 3. Differentially expressed miRNA in clear cell papillary renal cell carcinoma compared to normal matched tissue with log FC>2 and FDR (false discovery rate) <5%.

miRNA Name	CCPRCC	CCRCC	PRCC	Selected validated Targets
hsa-miR-122	UP	UP	NS	SLC7A1, GYS1, GTF2B
hsa-miR-15a	UP	UP	NS	BCL2, VEGFA, PDCD4
hsa-miR-18a	UP	UP	NS	BIM, CTGF, ESR1
hsa-miR-193a-3p	UP	UP	NS	E2F6, PTK2, MCL1
hsa-miR-1281	UP	NS	UP	-
hsa-miR-653	UP	NS	UP	-
hsa-miR-501-3p	DOWN	NS	DOWN	-
hsa-miR-532-3p	DOWN	NS	DOWN	-
hsa-miR-532-5p	DOWN	NS	DOWN	RUNX3

Table 4. Differentially expressed miRNAs among clear cell papillary renal cell carcinoma, clear cell renal cell carcinoma and papillary renal cell carcinoma.

DISCUSSION

Distinguishing clear cell papillary renal cell carcinoma from clear cell renal cell carcinoma is important, since the former has yet to be reported as having a malignant potential. As we said noted above, despite having distinctive morphological and immunohistochemical characteristics, these two entities can show overlapping features, resulting in diagnostic errors. In our study we have demonstrated that CK7 positivity and FISH evaluation for 3p deletion, although useful, might not be sufficient for distinguishing clear cell papillary renal cell carcinoma from conventional clear cell RCC.

Although clear cell papillary renal cell carcinoma was initially described as a multicystic neoplasm with a prominent papillary architecture and composed of cells with clear cytoplasm, subsequent series of this tumor have shown a broader spectrum of morphological features. Aydin and Williamson highlighted that the papillary component is present only in 81% and 65% of cases, emphasizing the branched tubular pattern, rather than the papillary pattern, as a distinctive morphological characteristic. This latter aspect, however, was often missing in tumors with a prominent cystic component [82,83].

These data underscore the difficulties that may be encountered in distinguishing this tumor from papillary renal cell carcinoma with prominent clearing of cytoplasm [84], as well as multicystic clear cell renal cell carcinoma and conventional clear cell renal cell carcinoma. Such difficulty has been clearly demonstrated by Williamson et al. who reported that 14 clear cell papillary renal cell carcinomas were identified from 469 renal cell carcinoma resections performed from 2004 to 2006 and that the majority of these tumors were originally diagnosed as clear cell renal cell carcinoma [82]. Their work reinforced the notion that there can be

substantial morphologic overlap between clear cell papillary RCC and conventional clear cell RCC as only a single tumor with an original diagnosis of papillary renal cell carcinoma was reclassified, while only three were originally interpreted as multilocular cystic renal cell carcinomas.

Recently, clear cell papillary renal cell carcinoma-like tumors in patients with or without Von Hippel-Lindau disease unrelated to sporadic clear cell papillary renal cell carcinoma have been described, highlighting once again the difficulties that one might encounter in distinguishing clear cell papillary renal cell carcinoma from conventional clear cell renal cell carcinoma [85,86].

In support of the diagnostic difficulties mentioned above, one of the tumors that we selected as clear cell papillary renal cell carcinoma, based on typical morphological and immunophenotypical features (diffuse papillary architecture with a characteristic arrangement of the nuclei, as well as the presence of branched tubules and CK7 positivity), proved to be a conventional clear cell carcinoma with alterations of 3p identified by array CGH and VHL mutation. This tumor showed a strong and diffuse immunoreactivity for CK7, a marker currently considered as extremely useful for differentiating clear cell papillary renal cell carcinoma from clear cell renal cell carcinoma [26,87].

Although the majority of clear cell renal cell carcinomas lack CK7 immunoexpression, some cases have been reported to be positive for this marker. We performed a literature search encompassing a total of 391 cases of clear cell renal cell carcinoma and found that 44 (12%) expressed CK7 [40,43,44,88]. Moreover, in our hands we have demonstrated this immunoreactivity in even more (24%) CCRCC.

As we demonstrated here, this might lead to misdiagnosis, even in the presence of morphologic features typical of clear cell papillary renal cell carcinoma.

34βE12 is an antibody that recognizes a different high molecular weight cytokeratins (CK) including CK 1, 5, 10 and 14; interestingly, we found 34βE12 to be positive in all but two cases (12/14, 86%), one of these being the CK7-positive CCRCC case. Rohan *et al*. showed 7/9 (78%) of their clear cell papillary renal cell carcinoma cases to be positive for this marker; on the other hand, 34βE12 immunostain was not detected in any of their clear cell renal cell carcinoma tested (0/11, 0%) [87] in this study. In our control group of clear cell RCC only 1% of the cases showed positivity for this marker. In order to better understand which specific cytokeratin is most responsible for the observed 34βE12 positivity in clear cell papillary renal cell carcinoma, we evaluated the immunoexpression of CK1, CK5, CK10 and CK14 separately. We found that, among these molecules, CK14 followed by CK5 are the most highly expressed high molecular weight cytokeratins in clear cell papillary renal cell carcinoma. We also evaluated the expression of CK14 in TMAs containing 150 cases of conventional clear cell renal cell carcinoma: only 2/150 cases (1%) stained weakly positive for the marker and showed the same pattern of expression of 34βE12. We therefore suggest that applying 34βE12, or alternatively CK14, to the immunohistochemical panel for diagnosing clear cell papillary renal cell carcinoma might be useful for distinguishing the latter from conventional clear cell renal cell carcinoma.

Among the most differentially expressed miRNA in CCPRCC, we found miR-210, miR-122, miR-34a, miR-21, miR-34b* and miR-489 to be upregulated while miR-4284, miR-1202, miR-135a, miR-1973 and miR-204 were downregulated compared to normal renal parenchyma.   Our microarray findings were further validated by qRT-PCR analysis in three of the most differentially expressed miRNAs. Our study also revealed that miRNA profile in CCPRCC is more similar to that of

CCRCC compared to PRCC. As expected, CCPRCC miRNA profile similarity was closer to that of primary than metastatic CCRCC.

At the molecular level, CCRCC is characterized by alteration of the *VHL* gene located at chromosome 3p25.3 in the majority of cases. Other common alterations involve copy number changes of chromosome 5q and a recently reported mutation of the SWI/SNF-related gene *PBRM1* [89-91]. None of these alterations have been seen in association with CCPRCC[26,87].

CAIX is upregulated by HIF. In CCRCC the latter is upregulated as a result of *VHL* loss of function (26, 27). Rohan et al. recently showed normal or elevated *VHL* mRNA expression in CCPRCC compared to normal control[87]. The authors concluded that a wide range of genetic, epigenetic and physiologic factors might be the cause for the activation of the HIF pathway that they encountered in this type of tumors. Several studies have documented miR-210 to be overexpressed miRNA in CCRCC[92]. MiR-210 is a well known target of HIF and a central player in hypoxia pathway[93]. A recent report also demonstrated that miRNA-210 expression positively modulates HIF and correlates with CAIX expression.[94] Intriguingly, our finding of miR-210 upregulation in CCPRCC could be implicating miR-210 in the activation of the hypoxia pathway in the absence of *VHL*. Evidently such hypothesis would require verification.

Among other miRNAs that we found upregulated in our CCPRCC tumors is miR-122. It has also been consistently reported to be overexpressed in CCRCC and been proposed as a potential regulator of *VHL* gene[95]. A recent study revealed higher miR-122 levels in primary compared to metastatic CCRCC[81]. However, its role in CCRCC pathogenesis remains to be fully determined.

MiR-34a has been previously shown to be up-regulated in CCRCC[96]. Using CCRCC cell lines, Yamamura et al. demonstrated that miR-34a suppressess *c-MYC* and its complexes and inhibits cell invasion, thus suggesting a role as a tumor suppressor in renal cancers[97]. The pathogenic significance, if any, of our observed miR-34a upregulation in CCPRCC should be further explored .

miR-18a was also among miRNAs that we found to be upregulated in CCPRCC and CCRCC in comparison with PRCC. The overexpression of miR-18a has already been reported in renal cancer[98]. In breast cancer, miR-18a is implicated in negative feedback regulation of ERα and is upregulated by *c-MYC*[99]. ERα has been recently demonstrated to be a proteasomal degradation target of the VHL protein in renal carcinoma cell lines[100]. In *VHL*-deficient conditions, like CCRCC, ERα is not sequestered and induces cell proliferation. Although in CCRCC setting, miR-18a upregulation could be related to ERα, this is less likely the case in CCPRCC given their lack of VHL alterations. Whether *c-MYC* upregulation via miR-210 inhibition of its antagonist MNT is responsible for miR-18a in CCPRCC remains to be determined.

We found a general down-regulation of miRNAs in CCRCC compared to CCPRCC. This is in line with the previously shown stepwise down-regulation of microRNA expression from normal to primary and metastatic tumors in renal cancer among other tumors[81]. Among the miRNAs that we found to be consistently down-regulated in primary and metastatic CCRCC are members of the miR-200 family that are thought to regulate the epithelial-mesenchymal transition in human tumorigenesis. miR-141 and miR-200c, which have been consistently shown to be down-regulated in CCRCC[81] were also found to be the down-regulated miRNA in our CCRCC dataset analysis. Their expression in CCPRCC was not significantly different from matched normal tissues. Whether the lack of down-regulation of such key microRNA, involved

in the incremental progression of malignant biologic behavior of CCRCC, may be in part related to the relatively indolent behavior of CCPRCC would require further investigation.

We found miR-135a and miR-204 to be downregulated in CCPRCC. MiR-135a has been recently reported to act as a tumor suppressor in RCC cell lines by targeting *c-MYC*[101]. Mikhaylova et al. recently showed that miR-204 is a *VHL*-regulated tumor suppressor acting by inhibiting macroautophagy, with LC3B as a direct and functional target in CCRCC specimens[102]. The mechanisms underlying miR-204 downregulation in CCPRCC merits further investigation, specifically in regards to the function of *VHL.* A limitation of the current study is our inability to perform functional studies due to the fact that cell lines for CCPRCC are not available.

Finally, we propose a wide morphological and molecular study of clear cell-papillary RCC to better understand its right collocation in the classification of the tumors of the kidney. Now days the frequency of this tumor is about 3%. All the case are characterized by a low nuclear grade, small tumor size, no necrosis and low mitotic activity. None case of recurrence or metastasis is known. The behavior of clear cell-papillary RCC appears to be indolent and this fact rises the idea that "carcinoma" could not be the right term for this entity. The fact that its incidence is higher in end-stage kidneys can suggest a reactive pathogenesis and this could explain the total lack of genetic alterations.

Sometime in pathology, a proliferation that seems a carcinoma is called "carcinoma" even if there is no proof of its malignant potential and it will be called "carcinoma" even if a proof of its aggressive behavior will never appear.

REFERENCES

1. Amin MB, Tamboli P, Javidan J, et al: Prognostic impact of histologic subtyping of adult renal epithelial neoplasms: an experience of 405 cases. Am J Surg Pathol 26:281-91, 2002

2. Cheville JC, Lohse CM, Zincke H, et al: Comparisons of outcome and prognostic features among histologic subtypes of renal cell carcinoma. Am J Surg Pathol 27:612-24, 2003

3. Delahunt B, Bethwaite PB, Nacey JN: Outcome prediction for renal cell carcinoma: evaluation of prognostic factors for tumours divided according to histological subtype. Pathology 39:459-65, 2007

4. Ficarra V, Righetti R, Martignoni G, et al: Prognostic value of renal cell carcinoma nuclear grading: multivariate analysis of 333 cases. Urol Int 67:130-4, 2001

5. Moch H, Gasser T, Amin MB, et al: Prognostic utility of the recently recommended histologic classification and revised TNM staging system of renal cell carcinoma: a Swiss experience with 588 tumors. Cancer 89:604-14, 2000

6. Eble JN, Sauter G, Epstein JI, et al: World Health Organization: Pathology and Genetics of Tumours of the Urinary System and Male Genital Organs. Lyon, IARC Press, 2004

7. Martignoni G, Brunelli M, Gobbo S, et al: Role of molecular markers in diagnosis and prognosis of renal cell carcinoma. Anal Quant Cytol Histol 29:41-9, 2007

8. Zhou M, Roma A, Magi-Galluzzi C: The usefulness of immunohistochemical markers in the differential diagnosis of renal neoplasms. Clin Lab Med 25:247-57, 2005

9.   Jones TD, Eble JN, Wang M, et al: Molecular genetic evidence for the independent origin of multifocal papillary tumors in patients with papillary renal cell carcinomas. Clin Cancer Res 11:7226-33, 2005

10.   Sanjmyatav J, Rubtsov N, Starke H, et al: Identification of tumor entities of renal cell carcinoma using interphase fluorescence in situ hybridization. J Urol 174:731-5, 2005

11.   Escudier B, Eisen T, Stadler WM, et al: Sorafenib in advanced clear-cell renal-cell carcinoma. N Engl J Med 356:125-34, 2007

12.   Denton MD, Magee CC, Ovuworie C, et al: Prevalence of renal cell carcinoma in patients with ESRD pre-transplantation: a pathologic analysis. Kidney Int 61:2201-9, 2002

13.   Hughson MD, Bigler S, Dickman K, et al: Renal cell carcinoma of end-stage renal disease: an analysis of chromosome 3, 7, and 17 abnormalities by microsatellite amplification. Mod Pathol 12:301-9, 1999

14.   Ikeda R, Tanaka T, Moriyama MT, et al: Proliferative activity of renal cell carcinoma associated with acquired cystic disease of the kidney: comparison with typical renal cell carcinoma. Hum Pathol 33:230-5, 2002

15.   Ishikawa I, Kovacs G: High incidence of papillary renal cell tumours in patients on chronic haemodialysis. Histopathology 22:135-9, 1993

16.   Khurana KK, Truong LD, Verani RR: Image analysis of proliferating cell nuclear antigen expression and immunohistochemical profiles in renal cell carcinoma associated with acquired cystic kidney disease: comparison with classic renal cell carcinoma. Mod Pathol 11:339-46, 1998

17.   Konda R, Sato H, Hatafuku F, et al: Expression of hepatocyte growth factor and its receptor C-met in acquired renal cystic disease associated with renal cell carcinoma. J Urol 171:2166-70, 2004

18.   Peces R, Martinez-Ara J, Miguel JL, et al: Renal cell carcinoma co-existent with other renal disease: clinico-pathological features in pre-dialysis patients and those receiving dialysis or renal transplantation. Nephrol Dial Transplant 19:2789-96, 2004

19.   Rioux-Leclercq NC, Epstein JI: Renal cell carcinoma with intratumoral calcium oxalate crystal deposition in patients with acquired cystic disease of the kidney. Arch Pathol Lab Med 127:E89-92, 2003

20.   Truong LD, Choi YJ, Shen SS, et al: Renal cystic neoplasms and renal neoplasms associated with cystic renal diseases: pathogenetic and molecular links. Adv Anat Pathol 10:135-59, 2003

21.   Eble J, Sauter G, Epstein J, et al: Tumours of the Kidney, in IARC (ed): World Health Organization Classification of Tumours: Pathology and Genetics of Tumours of the Urinary System and Male Genital Organs. Lyon, 2004

22.   Sule N, Yakupoglu U, Shen SS, et al: Calcium oxalate deposition in renal cell carcinoma associated with acquired cystic kidney disease: a comprehensive study. Am J Surg Pathol 29:443-51, 2005

23.   Tickoo SK, dePeralta-Venturina MN, Harik LR, et al: Spectrum of epithelial neoplasms in end-stage renal disease: an experience from 66 tumor-bearing kidneys with emphasis on histologic patterns distinct from those in sporadic adult renal neoplasia. Am J Surg Pathol 30:141-53, 2006

24.   Cossu-Rocca P, Eble JN, Zhang S, et al: Acquired cystic disease-associated renal tumors: an immunohistochemical and fluorescence in situ hybridization study. Mod Pathol 19:780-7, 2006

25.   O'Reilly KC, Tickoo SK, Amin MB, et al: Renal cell tumors arising in end stage renal disease (ESRD): a karyotypic study with fluorescent-in-situ-hybridization (FISH). Mod Pathol 18:156A, 2005

26.   Gobbo S, Eble JN, Grignon DJ, et al: Clear cell papillary renal cell carcinoma: a distinct histopathologic and molecular genetic entity. Am J Surg Pathol 32:1239-45, 2008

27.   Fuzesi L, Gunawan B, Bergmann F, et al: Papillary renal cell carcinoma with clear cell cytomorphology and chromosomal loss of 3p. Histopathology 35:157-61, 1999

28.   Salama ME, Worsham MJ, DePeralta-Venturina M: Malignant papillary renal tumors with extensive clear cell change: a molecular analysis by microsatellite analysis and fluorescence in situ hybridization. Arch Pathol Lab Med 127:1176-81, 2003

29.   Martignoni G, Pea M, Brunelli M, et al: CD10 is expressed in a subset of chromophobe renal cell carcinomas. Mod Pathol 17:1455-63, 2004

30.   Martignoni G, Pea M, Chilosi M, et al: Parvalbumin is constantly expressed in chromophobe renal carcinoma. Mod Pathol 14:760-7, 2001

31.   Leroy X, Moukassa D, Copin MC, et al: Utility of cytokeratin 7 for distinguishing chromophobe renal cell carcinoma from renal oncocytoma. Eur Urol 37:484-7, 2000

32.   Mathers ME, Pollock AM, Marsh C, et al: Cytokeratin 7: a useful adjunct in the diagnosis of chromophobe renal cell carcinoma. Histopathology 40:563-7, 2002

33.   Rocca PC, Brunelli M, Gobbo S, et al: Diagnostic utility of S100A1 expression in renal cell neoplasms: an immunohistochemical and quantitative RT-PCR study. Mod Pathol 20:722-8, 2007

34.   Tretiakova MS, Sahoo S, Takahashi M, et al: Expression of alpha-methylacyl-CoA racemase in papillary renal cell carcinoma. Am J Surg Pathol 28:69-76, 2004

35.   Brunelli M, Eble JN, Zhang S, et al: Eosinophilic and classic chromophobe renal cell carcinomas have similar frequent losses of multiple chromosomes from among chromosomes 1, 2, 6, 10, and 17, and this pattern of genetic abnormality is not present in renal oncocytoma. Mod Pathol 18:161-9, 2005

36.   Brunelli M, Eble JN, Zhang S, et al: Gains of chromosomes 7, 17, 12, 16, and 20 and loss of Y occur early in the evolution of papillary renal cell neoplasia: a fluorescent in situ hybridization study. Mod Pathol 16:1053-9, 2003

37.   Brunelli M, Eble JN, Zhang S, et al: Metanephric adenoma lacks the gains of chromosomes 7 and 17 and loss of Y that are typical of papillary renal cell carcinoma and papillary adenoma. Mod Pathol 16:1060-3, 2003

38.   Cossu-Rocca P, Eble JN, Delahunt B, et al: Renal mucinous tubular and spindle carcinoma lacks the gains of chromosomes 7 and 17 and losses of chromosome Y that are prevalent in papillary renal cell carcinoma. Mod Pathol 19:488-93, 2006

39.   Avery AK, Beckstead J, Renshaw AA, et al: Use of antibodies to RCC and CD10 in the differential diagnosis of renal neoplasms. Am J Surg Pathol 24:203-10, 2000

40.   Pan CC, Chen PC, Ho DM: The diagnostic utility of MOC31, BerEP4, RCC marker and CD10 in the classification of renal cell carcinoma and renal oncocytoma: an immunohistochemical analysis of 328 cases. Histopathology 45:452-9, 2004

41.   Holm-Nielsen P, Pallesen G: Expression of segment-specific antigens in the human nephron and in renal epithelial tumors. APMIS Suppl 4:48-55, 1988

42.   Ordonez NG: The diagnostic utility of immunohistochemistry in distinguishing between mesothelioma and renal cell carcinoma: a comparative study. Hum Pathol 35:697-710, 2004

43.   Skinnider BF, Folpe AL, Hennigar RA, et al: Distribution of cytokeratins and vimentin in adult renal neoplasms and normal renal tissue: potential utility of a cytokeratin antibody panel in the differential diagnosis of renal tumors. Am J Surg Pathol 29:747-54, 2005

44.   Kim MK, Kim S: Immunohistochemical profile of common epithelial neoplasms arising in the kidney. Appl Immunohistochem Mol Morphol 10:332-8, 2002

45.   Langner C, Wegscheider BJ, Ratschek M, et al: Keratin immunohistochemistry in renal cell carcinoma subtypes and renal oncocytomas: a systematic analysis of 233 tumors. Virchows Arch 444:127-34, 2004

46.   Langner C, Ratschek M, Rehak P, et al: Expression of MUC1 (EMA) and E-cadherin in renal cell carcinoma: a systematic immunohistochemical analysis of 188 cases. Mod Pathol 17:180-8, 2004

47.   Huo L, Sugimura J, Tretiakova MS, et al: C-kit expression in renal oncocytomas and chromophobe renal cell carcinomas. Hum Pathol 36:262-8, 2005

48.   Taki A, Nakatani Y, Misugi K, et al: Chromophobe renal cell carcinoma: an immunohistochemical study of 21 Japanese cases. Mod Pathol 12:310-7, 1999

49.   Liao SY, Aurelio ON, Jan K, et al: Identification of the MN/CA9 protein as a reliable diagnostic biomarker of clear cell carcinoma of the kidney. Cancer Res 57:2827-31, 1997

50.   Sandlund J, Oosterwijk E, Grankvist K, et al: Prognostic impact of carbonic anhydrase IX expression in human renal cell carcinoma. BJU Int 100:556-60, 2007

51.   Tamaskar I, Choueiri TK, Sercia L, et al: Differential expression of caveolin-1 in renal neoplasms. Cancer 110:776-82, 2007

52.   Steiner G, Sidransky D: Molecular differential diagnosis of renal carcinoma: from microscopes to microsatellites. Am J Pathol 149:1791-5, 1996

53.   Yamaguchi S, Yoshihiro S, Matsuyama H, et al: The allelic loss of chromosome 3p25 with c-myc gain is related to the development of clear-cell renal cell carcinoma. Clin Genet 63:184-91, 2003

54.   Nagao K, Yoshihiro S, Matsuyama H, et al: Clinical significance of allelic loss of chromosome region 5q22.3 approximately q23.2 in nonpapillary renal cell carcinoma. Cancer Genet Cytogenet 136:23-30, 2002

55.   Herbers J, Schullerus D, Muller H, et al: Significance of chromosome arm 14q loss in nonpapillary renal cell carcinomas. Genes Chromosomes Cancer 19:29-35, 1997

56.   Brunelli M, Eccher A, Gobbo S, et al: Loss of chromosome 9p is an independent prognostic factor in patients with clear cell renal cell carcinoma. Mod Pathol 21:1-6, 2008

57.   Delahunt B, Eble JN: Papillary renal cell carcinoma: a clinicopathologic and immunohistochemical study of 105 tumors. Mod Pathol 10:537-44, 1997

58.   Delahunt B, Eble JN: Papillary renal cell carcinoma: a clinicopathologic and immunohistochemical study of 105 tumors. Mod Pathol 10:537-44, 1997

59.   Leroy X, Zini L, Leteurtre E, et al: Morphologic subtyping of papillary renal cell carcinoma: correlation with prognosis and differential expression of MUC1 between the two subtypes. Mod Pathol 15:1126-30, 2002

60.   Olgac S, Hutchinson B, Tickoo SK, et al: Alpha-methylacyl-CoA racemase as a marker in the differential diagnosis of metanephric adenoma. Mod Pathol 19:218-24, 2006

61.   McGregor DK, Khurana KK, Cao C, et al: Diagnosing primary and metastatic renal cell carcinoma: the use of the monoclonal antibody 'Renal Cell Carcinoma Marker'. Am J Surg Pathol 25:1485-92, 2001

62.   Kunju LP, Wojno K, Wolf JS, Jr., et al: Papillary renal cell carcinoma with oncocytic cells and nonoverlapping low grade nuclei: expanding the morphologic spectrum with emphasis on clinicopathologic, immunohistochemical and molecular features. Hum Pathol 39:96-101, 2008

63.   Jiang F, Richter J, Schraml P, et al: Chromosomal imbalances in papillary renal cell carcinoma: genetic differences between histological subtypes. Am J Pathol 153:1467-73, 1998

64.   Henke RP, Erbersdobler A: Numerical chromosomal aberrations in papillary renal cortical tumors: relationship with histopathologic features. Virchows Arch 440:604-9, 2002

65.   Jiang F, Richter J, Schraml P, et al: Chromosomal imbalances in papillary renal cell carcinoma: genetic differences between histological subtypes. Am J Pathol 153:1467-73, 1998

66.   Hes O, Brunelli M, Michal M, et al: Oncocytic papillary renal cell carcinoma: a clinicopathologic, immunohistochemical, ultrastructural, and interphase cytogenetic study of 12 cases. Ann Diagn Pathol 10:133-9, 2006

67.   Cossu-Rocca P, Zhang S, Roth LM, et al: Chromosome 12p abnormalities in dysgerminoma of the ovary: a FISH analysis. Mod Pathol 19:611-5, 2006

68.   Kernek KM, Brunelli M, Ulbright TM, et al: Fluorescence in situ hybridization analysis of chromosome 12p in paraffin-embedded tissue is useful for establishing germ cell origin of metastatic tumors. Mod Pathol 17:1309-13, 2004

69.   Brunelli M, Eble JN, Zhang S, et al: Metanephric adenoma lacks the gains of chromosomes 7 and 17 and loss of Y that are typical of papillary renal cell carcinoma and papillary adenoma. Mod Pathol 16:1060-3, 2003

70.   Brunelli M, Eble JN, Zhang S, et al: Gains of chromosomes 7, 17, 12, 16, and 20 and loss of Y occur early in the evolution of papillary renal cell neoplasia: a fluorescent in situ hybridization study. Mod Pathol 16:1053-9, 2003

71.   Fallon KB, Palmer CA, Roth KA, et al: Prognostic value of 1p, 19q, 9p, 10q, and EGFR-FISH analyses in recurrent oligodendrogliomas. J Neuropathol Exp Neurol 63:314-22, 2004

72.   van Houwelingen KP, van Dijk BA, Hulsbergen-van de Kaa CA, et al: Prevalence of von Hippel-Lindau gene mutations in sporadic renal cell carcinoma: results from The Netherlands cohort study. BMC Cancer 5:57, 2005

73.   Choueiri TK, Vaziri SA, Jaeger E, et al: von Hippel-Lindau gene status and response to vascular endothelial growth factor targeted therapy for metastatic clear cell renal cell carcinoma. J Urol 180:860-5; discussion 865-6, 2008

74.   Nygren AO, Ameziane N, Duarte HM, et al: Methylation-specific MLPA (MS-MLPA): simultaneous detection of CpG methylation and copy number changes of up to 40 sequences. Nucleic Acids Res 33:e128, 2005

75.   Coffa J, van de Wiel MA, Diosdado B, et al: MLPAnalyzer: data analysis tool for reliable automated normalization of MLPA fragment data. Cell Oncol 30:323-35, 2008

76.   Zhan H, Cardozo C, Yu W, et al: MicroRNA deregulation in polycythemia vera and essential thrombocythemia patients. Blood Cells Mol Dis 50:190-5, 2013

77.   Livak KJ, Schmittgen TD: Analysis of relative gene expression data using real-time quantitative PCR and the 2(-Delta Delta C(T)) Method. Methods 25:402-8, 2001

78.   Benassi B, Flavin R, Marchionni L, et al: MYC is activated by USP2a-mediated modulation of microRNAs in prostate cancer. Cancer Discov 2:236-47, 2012

79.   Schaeffer EM, Marchionni L, Huang Z, et al: Androgen-induced programs for prostate epithelial growth and invasion arise in embryogenesis and are reactivated in cancer. Oncogene 27:7180-91, 2008

80.   Ross AE, Marchionni L, Vuica-Ross M, et al: Gene expression pathways of high grade localized prostate cancer. Prostate, 2011

81.   Wotschofsky Z, Liep J, Meyer HA, et al: Identification of metastamirs as metastasis-associated microRNAs in clear cell renal cell carcinomas. Int J Biol Sci 8:1363-74, 2012

82.   Williamson SR, Eble JN, Cheng L, et al: Clear cell papillary renal cell carcinoma: differential diagnosis and extended immunohistochemical profile. Mod Pathol, 2012

83.   Aydin H, Chen L, Cheng L, et al: Clear cell tubulopapillary renal cell carcinoma: a study of 36 distinctive low-grade epithelial tumors of the kidney. Am J Surg Pathol 34:1608-21, 2010

84.   Gobbo S, Eble JN, Maclennan GT, et al: Renal cell carcinomas with papillary architecture and clear cell components: the utility of immunohistochemical and cytogenetical analyses in differential diagnosis. Am J Surg Pathol 32:1780-6, 2008

85.   Williamson S, Zhang S, Eble J, et al: Clear cell papillary renal cell carcinoma-like tumors in patients with Von Hippel-Lindau disease are unrelated to sporadic clear cell papillary renal cell carcinoma. Am J Surg Pathol In Press, 2013

86.   Petersson F, Grossmann P, Hora M, et al: Renal cell carcinoma with areas mimicking renal angiomyoadenomatous tumor/clear cell papillary renal cell carcinoma. Hum Pathol 44:1412-20, 2013

87.   Rohan SM, Xiao Y, Liang Y, et al: Clear-cell papillary renal cell carcinoma: molecular and immunohistochemical analysis with emphasis on the von Hippel-Lindau gene and hypoxia-inducible factor pathway-related proteins. Mod Pathol 24:1207-20, 2011

88.   Ohta Y, Suzuki T, Shiokawa A, et al: Expression of CD10 and cytokeratins in ovarian and renal clear cell carcinoma. Int J Gynecol Pathol 24:239-45, 2005

89.   Varela I, Tarpey P, Raine K, et al: Exome sequencing identifies frequent mutation of the SWI/SNF complex gene PBRM1 in renal carcinoma. Nature 469:539-42, 2011

90.   Kovacs G, Erlandsson R, Boldog F, et al: Consistent chromosome 3p deletion and loss of heterozygosity in renal cell carcinoma. Proc Natl Acad Sci U S A 85:1571-5, 1988

91.   Eble JN, Sauter G, Epstein JI, et al: Tumours of the kidney, World Health Organization Classification of Tumours: Pathology and Genetics of Tumours of the Urinary System and Male Genital Organs. Lyon, IARC Press, 2004

92.   Slaby O, Redova M, Poprach A, et al: Identification of MicroRNAs associated with early relapse after nephrectomy in renal cell carcinoma patients. Genes Chromosomes Cancer 51:707-16, 2012

93.   Chan SY, Loscalzo J: MicroRNA-210: a unique and pleiotropic hypoxamir. Cell Cycle 9:1072-83, 2010

94.   Chang W, Lee CY, Park JH, et al: Survival of hypoxic human mesenchymal stem cells is enhanced by a positive feedback loop involving miR-210 and hypoxia-inducible factor 1. J Vet Sci 14:69-76, 2013

95.   Zhou L, Chen J, Li Z, et al: Integrated profiling of microRNAs and mRNAs: microRNAs located on Xq27.3 associate with clear cell renal cell carcinoma. PLoS One 5:e15224, 2010

96.	Osanto S, Qin Y, Buermans HP, et al: Genome-wide microRNA expression analysis of clear cell renal cell carcinoma by next generation deep sequencing. PLoS One 7:e38298, 2012

97.	Yamamura S, Saini S, Majid S, et al: MicroRNA-34a suppresses malignant transformation by targeting c-Myc transcriptional complexes in human renal cell carcinoma. Carcinogenesis 33:294-300, 2012

98.	Neal CS, Michael MZ, Rawlings LH, et al: The VHL-dependent regulation of microRNAs in renal cancer. BMC Med 8:64, 2010

99.	Castellano L, Giamas G, Jacob J, et al: The estrogen receptor-alpha-induced microRNA signature regulates itself and its transcriptional response. Proc Natl Acad Sci U S A 106:15732-7, 2009

100.	Jung YS, Lee SJ, Yoon MH, et al: Estrogen receptor alpha is a novel target of the Von Hippel-Lindau protein and is responsible for the proliferation of VHL-deficient cells under hypoxic conditions. Cell Cycle 11:4462-73, 2012

101.	Yamada Y, Hidaka H, Seki N, et al: Tumor-suppressive microRNA-135a inhibits cancer cell proliferation by targeting the c-MYC oncogene in renal cell carcinoma. Cancer Sci 104:304-12, 2013

102.	Mikhaylova O, Stratton Y, Hall D, et al: VHL-regulated MiR-204 suppresses tumor growth through inhibition of LC3B-mediated autophagy in renal clear cell carcinoma. Cancer Cell 21:532-46, 2012